iScience

CellPress
OPEN ACCESS

Article

The Hsp40 Mas5 Connects Protein Quality Control and the General Stress Response through the Thermo-sensitive Pyp1

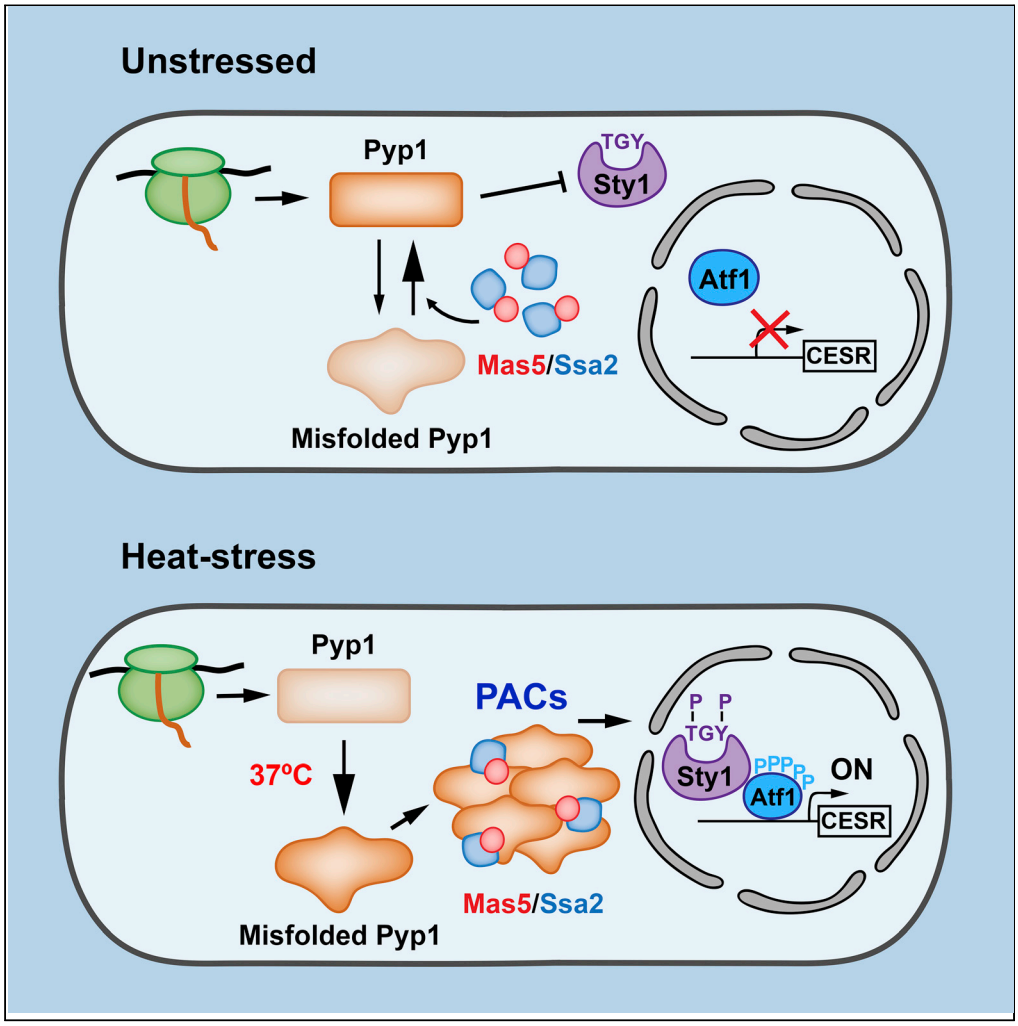

Susanna Boronat, Luis Marte, Montserrat Vega, Sarela García-Santamarina, Margarita Cabrera, José Ayté, Elena Hidalgo

elena.hidalgo@upf.edu

HIGHLIGHTS

Pyp1 phosphatase requires Mas5 to escape from degradation in unstressed conditions

Pyp1 assembles into protein aggregate centers (PACs) upon temperature up-shifts

Temporal sequestration of Pyp1 into PACs upon heat shock allows Sty1 activation

Pyp1 incorporation into PACs depends on Mas5

Boronat et al., iScience *23*, 101725
November 20, 2020
https://doi.org/10.1016/j.isci.2020.101725

iScience

CellPress
OPEN ACCESS

Article

The Hsp40 Mas5 Connects Protein Quality Control and the General Stress Response through the Thermo-sensitive Pyp1

Susanna Boronat,[1] Luis Marte,[1] Montserrat Vega,[1] Sarela García-Santamarina,[1,2] Margarita Cabrera,[1] José Ayté,[1] and Elena Hidalgo[1,3,*]

SUMMARY

Upon heat shock, the fission yeast Hsp40 chaperone Mas5 drives temperature-sensitive proteins toward protein aggregate centers (PACs) to avoid their degradation until lower temperatures favor their refolding. We show here that cells lacking Mas5 are resistant to oxidative stress. Components of the general stress pathways, the MAP kinase Sty1 and the transcription factor Atf1, are suppressors of this phenotype. Strain *Δmas5* expresses higher levels of Sty1- and Atf1-dependent stress genes than wild-type cells. Pyp1, the main tyrosine phosphatase maintaining Sty1 inactive in the absence of stress, is a temperature-sensitive protein that aggregates upon temperature up-shifts in a Mas5-dependent manner. In strain *Δmas5*, Pyp1 is sent to proteasomal degradation even in the absence of stress. We propose that Pyp1 is a thermo-sensitive phosphatase, which during heat stress coalescences into PACs in a Mas5-dependent manner, to promote full activation of the anti-stress Sty1-Atf1 cascade.

INTRODUCTION

Protein homeostasis, also known as proteostasis, is continuously challenged during the process of protein synthesis, where non-productive interactions can compromise the formation of the final native structure, and during heat shock and other stresses. The protein quality control (PQC) system assists proteins during their synthesis to avoid misfolding, and participates in refolding, but also degrades aberrant proteins. Once synthesized, proteins also require PQC components to be maintained in their native conformations, and the PQC system is particularly challenged by environmental situations such as oxidative or metal stress and, in particular, heat shock. Thus, chaperones of different families assist proteins in a co-translational or post-translational manner (for reviews, see Hipp et al., 2019; Jayaraj et al., 2020; Kim et al., 2013; Pilla et al., 2017).

In particular, heat shock protein (Hsp)70-based complexes execute diverse roles in PQC, the main one being folding of proteins (for reviews, see Craig and Marszalek, 2017; Kampinga and Craig, 2010; Liu et al., 2020). These complexes interact with hydrophobic stretches of residues in proteins, and this interaction depends on nucleotides (ATP and ADP). The partners of Hsp70s, known as J-proteins or Hsp40s, directly interact with the client proteins and control the rate of ATP hydrolysis in the Hsp70s, whereas nucleotide exchange factors regulate the exchange of ADP with ATP. Many are the functions assigned to Hsp70/40 machines, in general (with a broad range of protein substrates) and in specific (with a limited number of clients) cellular processes. Based on sequence comparisons, the fission yeast genome encodes eight putative Hsp70 proteins and 17 Hsp40 chaperones, among them Mas5 (Craig and Marszalek, 2017; Kominek et al., 2013).

Mas5 is the homolog of the budding yeast Hsp40 Ydj1. In fission yeast, Mas5 has been proposed to participate in mitochondrial homeostasis (Kim et al., 2010) and in heterochromatin assembly (Okazaki et al., 2018), and a direct participation in proteostasis control has been reported by the Oliferenko lab (Vjestica et al., 2013). According to their work, Mas5 negatively regulates the heat shock factor Hsf1, so that cells lacking Mas5 display constitutive activation of this important transcription factor and its downstream genes.

We have recently unraveled another important function of Mas5: during heat shock the Hsp40/70 couple Mas5/Ssa2 drives non-terminally misfolded proteins to protein aggregate centers (PACs) (Cabrera et al.,

[1]Oxidative Stress and Cell Cycle Group, Universitat Pompeu Fabra, C/ Dr. Aiguader 88, 08003 Barcelona, Spain

[2]Present address: European Molecular Biology Laboratory, Heidelberg, Meyerhofstraβe 1, Heidelberg, 69117, Germany

[3]Lead Contact

*Correspondence: elena.hidalgo@upf.edu

https://doi.org/10.1016/j.isci.2020.101725

2020). Protein aggregation, which can be visualized in different model systems thanks to the use of temperature-sensitive alleles fused to fluorescent tags, can appear in organized cellular inclusions, and their fate and roles are a matter of debate. Aggregates have been long associated to toxicity and are considered a hallmark of many neurodegenerative diseases. However, this link has been challenged by different reports suggesting that the formation of protein aggregation-like foci is a chaperone-mediated process to facilitate the deposit of non-native polypeptides into defined sub-cellular locations (Escusa-Toret et al., 2013; Miller et al., 2015; Sontag et al., 2017); the most popular hypothesis about the role of these deposits is that spatial sequestration of the aggregating protein intermediates separates them from the healthy native proteome. In fission yeast, the Mas5-dependent sequestration of misfolded clients into these discrete foci, the PACs, helps them escape from degradation (Cabrera et al., 2020). Thus, all the thermo-sensitive proteins present in the fission yeast proteome form non-terminal misfolding intermediates upon heat shock, and the Hsp40/70 couple Mas5/Ssa2 contributes to the assembly of these intermediates into PACs. These structures also contain numerous chaperones including Hsp104, which is required for the disassembly of PACs once physiological temperatures are recovered (Cabrera et al., 2020).

Besides spatial sequestration of non-native intermediates in discrete foci, another strategy to survive heat shock is the activation of signaling cascades and downstream transcriptional activation of anti-stress responses, namely, those of the transcription factor Hsf1 (kept inactive by Mas5/Ssa2 at basal temperatures, Vjestica et al., 2013) and of the Sty1 MAP kinase cascade (Chen et al., 2003). The Sty1 cascade responds to multiple environmental signals, and heat shock was proposed to inhibit the interaction of Sty1 with Pyp1, the main tyrosine phosphatase of this MAP kinase that dephosphorylates Sty1 under low-temperature conditions; the transient inhibition of this interaction leads to sustained activation of Sty1 upon heat stress (Nguyen and Shiozaki, 1999). The main substrate of activated Sty1 is the transcription factor Atf1, which then triggers a survival gene expression program (Chen et al., 2003; Salat-Canela et al., 2017; Wilkinson et al., 1996).

In a genetic screen to search for PQC components required for wild-type tolerance to oxidative stress in fission yeast (Marte et al., 2020), we have isolated *Δmas5* as a deletion strain unable to accumulate H_2O_2-dependent protein carbonyls, and as a consequence displaying resistance to oxidative stress. We show here that components of the Sty1 MAP kinase anti-stress cascade, but not of the Hsf1 pathway, are suppressors of these phenotypes. Detailed analyses of the transcriptome of cells lacking Mas5 demonstrate that not only the Hsf1-dependent gene expression program but also the Sty1-Atf1 cascade is constitutively engaged in *Δmas5*. We show that Pyp1 assembles into PACs upon heat shock in a Mas5-dependent manner, explaining its transient sequestration during heat stress and the release of basal Sty1 inhibition. Pyp1 is probably an intrinsically disordered protein, which naturally misfolds upon heat shock, and requires Mas5/Ssa2 assistance to avoid its degradation under normal growth conditions. The low levels of Pyp1 in a *Δmas5* strain explain the basal activation of the Sty1 gene expression program and the tolerance to oxidative stress. These phenotypes can be suppressed by over-expressing Pyp1. Our experiments demonstrate that Pyp1 is a cellular thermosensor, which becomes transiently inactivated by heat stress due to its intrinsic propensity to misfold and its recruitment into PACs.

RESULTS

Cells Lacking the Hsp40 Mas5 Display Severe Growth Defects but Are Resistant to Oxidative Stress

One of the hallmarks of oxidative stress toxicity is protein carbonylation. To assess the levels of protein carbonyls, extracts from cells exposed or not to toxic concentrations of peroxides were derivatized with fluorescein-5-thiosemicarbazide and monitored by poly-acrylamide electrophoresis followed by scanning fluorescence (Figure 1A). Thus, whole-cell extracts of wild-type cells display basal levels of protein carbonyls, which are dramatically exacerbated if cells have previously been exposed to toxic concentrations of H_2O_2 (Figure 1B, WT [wild type]).

In a biochemical screen of ~74 *S. pombe* deletion mutants whose gene products are components of the PQC system, we identified *mas5* as a strong suppressor of the accumulation of protein carbonyls in extracts from cells exposed to H_2O_2 (Figure 1B). This Hsp40 chaperone normally executes its roles with the Hsp70 protein Ssa2 (Cabrera et al., 2020; Vjestica et al., 2013). As shown in Figure 1C, extracts from cells lacking Ssa2, but not its homolog Ssa1, also display a severe reduction of H_2O_2-dependent protein carbonyls.

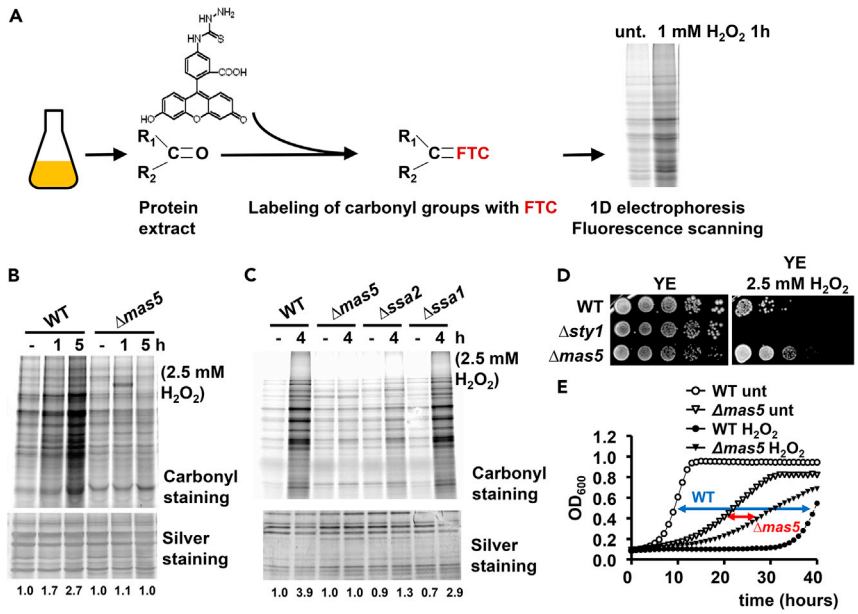

Figure 1. Cells Lacking the Hsp40 Mas5 Display Enhanced Tolerance to Oxidative Stress

(A) Scheme depicting the experimental procedure to analyze total protein carbonyls. Protein extracts from untreated (unt.) or H_2O_2-treated cells are derivatized with fluorescein-5-thiosemicarbazide (FTC) and analyzed by SDS-PAGE and fluorescence scanning. See Transparent Methods for details.

(B and C) Cells lacking the Hsp40 Mas5 or the Hsp70 Ssa2 do not accumulate protein carbonyls upon oxidative stress. Protein carbonyls were analyzed and quantified as indicated in Transparent Methods from strains 972 (WT), SB26 (*Δmas5*), SG289 (*Δssa2*), and SB291 (*Δssa1*) treated or not with 2.5 mM H_2O_2 for 1 and 5 h (B) or 4 h (C). Silver staining of gels was used as loading control.

(D and E) Cells lacking Mas5 show increased resistance to H_2O_2 on solid or liquid media. (D) Serial dilutions of strains 972 (WT), AV18 (*Δsty1*, used as a H_2O_2-sensitive control strain), and SB26 (*Δmas5*) were spotted on YE plates containing or not H_2O_2 and incubated for 2 (unt.) or 4 (H_2O_2) days. (E) Growth of YE cultures of 972 (WT) and SB26 (*Δmas5*) in the absence or presence of 2.5 mM H_2O_2 was monitored during 40 h by reading the OD_{600}. Double arrows indicate the lag time between untreated and H_2O_2-treated conditions to reach OD_{600}~0.5, blue for WT and red for *Δmas5* cells. Data represent the average of three independent experiments. See Figure S1C for the complete dataset with error bars.

See also Figure S1.

Mas5 is required to maintain the transcription factor Hsf1 inactive when cells are grown at low temperatures. Constitutive activation of Hsf1 is deleterious for growth, and as expected the strain *Δmas5* displays severe growth defects in the absence of added stressors, both on solid plates and in liquid cultures (Figures 1D and 1E). Mas5 is also required to catalyze the formation of PACs during heat shock; as expected, cells lacking this Hsp40 chaperone are more sensitive to grow at 37°C than wild-type cells (Figures S1A and S1B). Regarding oxidative stress, the H_2O_2 concentrations used to detect protein carbonylation are toxic to wild-type cells (Figures 1D and 1E). On the contrary, cells lacking Mas5 are tolerant to the addition of these toxic concentrations, as shown both on solid plates (Figure 1D) and liquid cultures (Figures 1E and S1C). As expected, cells lacking Ssa2 also display partial resistance to H_2O_2 (Figure S1D). We conclude that cells lacking Mas5 are more sensitive to heat shock than wild-type cells but display enhanced survival when exposed to peroxides.

Components of the Sty1 MAP Kinase Pathway Are Suppressors of the Oxidative Stress-Resistant Phenotype of Strain *Δmas5*

To decipher the role of Mas5 in oxidative stress tolerance, we searched for suppressors of the lack of protein carbonylation in extracts of *Δmas5* cells. As cells lacking Mas5 have been described to release the transcription factor Hsf1 and to display constitutive activation of its downstream genes (Vjestica et al., 2013) (Figure S2A), we tested the participation of the Hsf1 cascade on oxidative stress. One of the Hsf1-regulated genes is *hsp104*, coding for the high-molecular-weight chaperone Hsp104, and we confirmed by northern blot that its mRNA is highly expressed in cells lacking either Mas5 or Ssa2 (Figure S2B). The up-regulation of

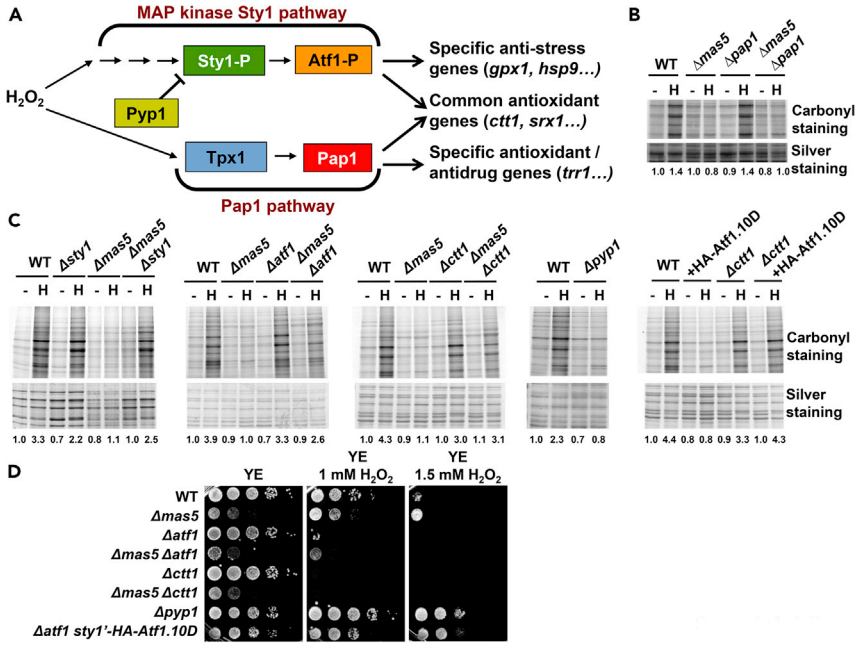

Figure 2. Components of the Sty1 MAP Kinase Pathway are Suppressors of the *Δmas5* Phenotypes

(A) Scheme depicting the two main pathways in *S. pombe* in response to oxidative stress. The main components of the MAP kinase Sty1 and the Pap1 pathways, activated by high and low levels of H_2O_2, respectively, are indicated. Some downstream activated genes are also indicated.

(B) The *pap1* gene is not a suppressor of *Δmas5*. Protein carbonyls in extracts of strains 972 (WT), SB26 (*Δmas5*), AV25 (*Δpap1*), and SG301 (*Δmas5 Δpap1*), treated or not with 2.5 mM H_2O_2 for 4 h, were analyzed and quantified as in Figure 1C.

(C) *sty1*, *atf1*, and *ctt1* are suppressors of *Δmas5*. Protein carbonyls in extracts of strains 972 (WT), AV18 (*Δsty1*), SB26 (*Δmas5*), SB234 (*Δmas5 Δsty1*), MS98 (*Δatf1*), SB319 (*Δmas5 Δatf1*), EP198 (*Δctt1*), SB245 (*Δmas5 Δctt1*), EP48 (*Δpyp1*), EP203.10D (expressing the constitutively active Atf1.10D), and SB464.10D (*Δctt1* expressing Atf1.10D), treated or not with 2.5 mM H_2O_2 for 4 h, were analyzed and quantified as in Figure 1C.

(D) YE cultures of strains 972 (WT), SB26 (*Δmas5*), MS98 (*Δatf1*), SB319 (*Δmas5 Δatf1*), EP198 (*Δctt1*), SB245 (*Δmas5 Δctt1*), EP48 (*Δpyp1*), and EP203.10D (expressing the constitutively active Atf1.10D) were spotted on YE plates containing the indicated concentrations of H_2O_2 and incubated at 30°C for 2 (unt.) or 3 days (H_2O_2).

See also Figure S2.

hsp104 is not involved in the absence of protein carbonyls in extracts from strain *Δmas5*, because cells lacking both Mas5 and Hsp104 do not accumulate oxidized proteins upon H_2O_2 treatment (Figure S2C). As Hsf1 is an essential protein, we expressed the *hsf1* gene under the control of the uracil-regulated *urg1* promoter in a *Δmas5* background (Vjestica et al., 2013) (Figure S2D), to test whether extracts from *Δmas5* cells expressing lower (wild-type) levels of Hsf1 were still unable to accumulate protein carbonyls. As shown in Figure S2E, even in the absence of Hsf1 over-activation (-U sample), cells lacking Mas5 are unable to accumulate protein carbonyls. Furthermore, wild-type cells expressing Hsf1 upon uracil addition (*urg1'::hsf1* in Figure S2F) have the same sensitivity to added peroxides than wild-type cells. In conclusion, *hsf1* is not a suppressor of the oxidative stress-resistant phenotype of *Δmas5*.

The two main cascades that respond to elevated H_2O_2 in fission yeast are the Tpx1-Pap1 and the Sty1-Atf1 pathways. Upon activation, the Pap1 and Atf1 transcription factors bind and trigger specific and common anti-stress genes (Figure 2A). Constitutive activation of the Pap1 pathway did not seem to cause the H_2O_2-resistant phenotype of cells lacking Mas5, as extracts from cells lacking both the Hsp40 and Pap1 still display lack of accumulation of protein carbonyls upon H_2O_2 addition to the cultures (Figure 2B), and cells lacking both Mas5 and Pap1 are much more resistant to oxidative stress than *Δpap1* cells (Figure S2G). On the contrary, several genes of the Sty1-Atf1 cascade, such as *sty1*, *atf1*, and *ctt1*, are clear suppressors of the *Δmas5* phenotypes, so that double deletion mutants do accumulate carbonylated proteins in their extracts (Figure 2C) and are no longer resistant to oxidative stress (Figure 2D). In fact, extracts from cells lacking Pyp1, the phosphatase maintaining Sty1 inactive in the absence of stress (Figure 2A), or from cells

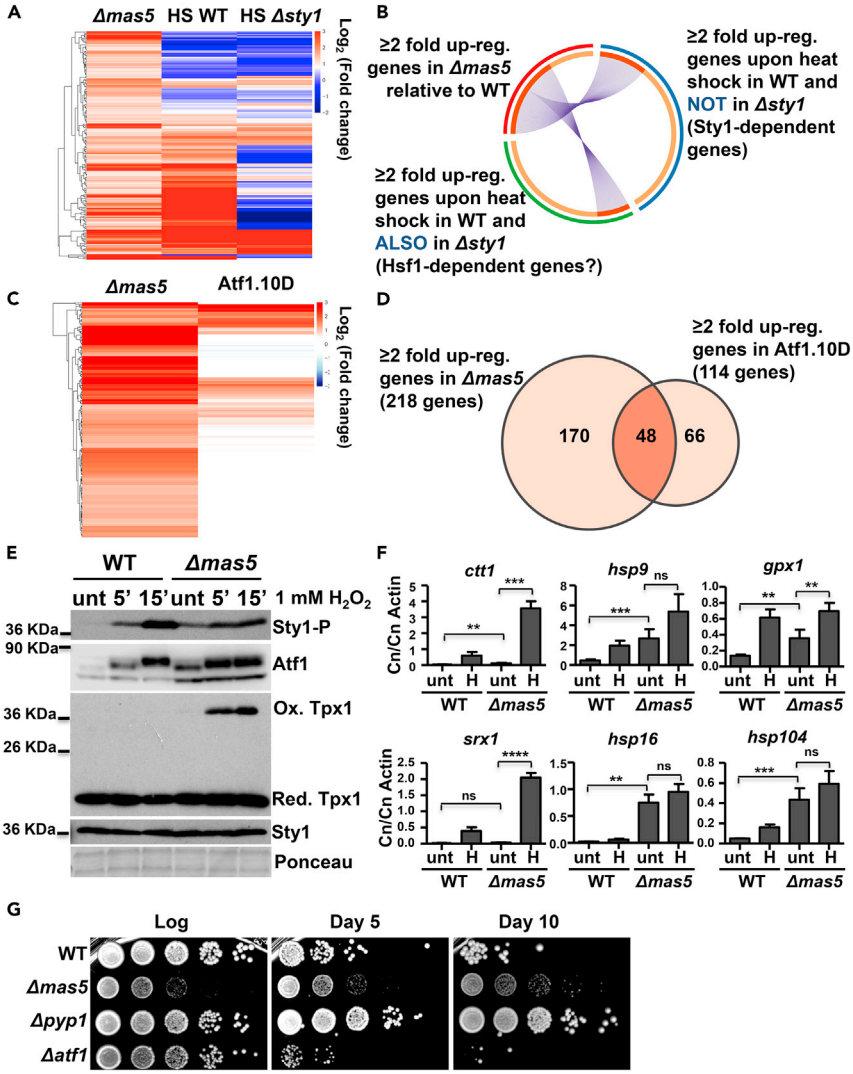

Figure 3. The MAP Kinase Sty1 Pathway Is De-repressed in Cells Lacking Mas5

(A) The transcriptome of cells lacking Mas5 partially recapitulates the transcriptional response to heat shock. Heatmap analysis comparing the ≥2-fold up-regulated genes in *Δmas5* cells identified by Vjestica et al. (2013) with the gene expression profile of wild-type and *Δsty1* cells upon heat shock published by Chen et al. (2003), expressed as Log_2 fold change.

(B) Different sets of genes up-regulated in *Δmas5* cells belong to different heat shock transcriptional programs. Circos plot representation of 187 genes up-regulated ≥2-fold in *Δmas5* cells (Vjestica et al., 2013) (in red), 287 genes up-regulated ≥2-fold by heat shock in a Sty1-dependent manner (in blue), and 222 genes up-regulated ≥2-fold by heat shock in a Sty1-independent manner (Chen et al., 2003) (in green) using the web-based analysis resource Metascape (Zhou et al., 2019).

(C and D) The transcriptome of *Δmas5* partially overlaps with that of cells expressing the constitutively active Atf1.10D. (C) Heatmap analysis comparing the ≥2-fold up-regulated genes in *Δmas5* cells identified by Vjestica et al. (2013) with the gene expression profile of unstressed Atf1.10D (Salat-Canela et al., 2017) expressed as Log_2 fold change. (D) Venn diagram shows the overlap of ≥2-fold up-regulated genes between *Δmas5* and Atf1.10D cells.

(E) Cells lacking Mas5 respond more readily to oxidative stress. Atf1 and Sty1 phosphorylation and Tpx1 oxidation were examined in 972 (WT) and SB26 (*Δmas5*) cells treated with H_2O_2 by western blot of tricarboxylic acid (TCA) extracts using Atf1-, phospho-p38 (Sty1-P)-, Tpx1-, and Sty1-specific antibodies. Sty1 and Ponceau were used as loading controls.

(F) Sty1- and Hsf1-dependent transcriptional programs are de-repressed in cells lacking Mas5. The mRNA levels of Sty1-dependent (*ctt1*, *hsp9*, *gpx1*, and *srx1*) and Hsf1-dependent (*hsp16* and *hsp104*) genes from 972 (WT) and SB26 (*Δmas5*) cells untreated or treated with 1 mM H_2O_2 (H) for 15 min were determined by RT-qPCR. Data are expressed as the mRNA copy number (Cn) relative to actin Cn and represent the average of at least three biological replicates. Error bars represent the S.D. (standard deviation). Statistical significance was calculated between the indicated samples with an

Figure 3. *Continued*
unpaired Student's t test and 95% confidence level with p values of 0.05 (*), 0.01, (**), 0.001 (***), and 0.0001 (****). ns, nonsignificant.
(G) Cells lacking Mas5 have an extended lifespan. Viability of YE cultures at the logarithmic phase or 5-10 days after reaching stationary phase of strains 972 (WT), SB26 (*Δmas5*), EP48 (*Δpyp1*), and MS98 (*Δatf1*) was analyzed by spot assay. Plates were incubated at 30°C for 2–5 days.
See also Figure S3.

expressing a constitutively active Atf1 mutant (Atf1.10D) (Salat-Canela et al., 2017), do not display accumulation of protein carbonyls upon H_2O_2 treatment (Figure 2C). Expression of Atf1.10D in a *Δctt1* background did not prevent the accumulation of carbonylated proteins, indicating that enhanced catalase levels are preventing protein oxidation (Figure 2C). These genetic experiments suggest that the enhanced oxidative stress tolerance of cells lacking Mas5 is totally dependent on the Sty1-Atf1 pathway.

The Sty1-Dependent Stress Response Is Partially Engaged in Cells Lacking Mas5 in the Absence of Stress Signals

The transcriptome of *Δmas5* cells may shed light on the molecular bases of the enhanced tolerance to peroxides. As mentioned above, RNA sequencing data from the laboratory of Oliferenko demonstrated that in cells lacking Mas5 many genes are constitutively engaged, whereas in wild-type cells those genes are only up-regulated upon heat shock through the activation of the Hsf1 transcription factor (Vjestica et al., 2013). In their study, Oliferenko and colleagues already suggested that other pathways could be also involved in the constitutive transcriptome signature of *Δmas5* strain, because less than half of the genes up-regulated in the chaperone mutant were also up-regulated upon Hsf1 over-expression (Vjestica et al., 2013). As described by the Bahler laboratory, the heat shock response is partially dependent on the general stress response pathway driven by Sty1-Atf1 (Chen et al., 2003). In cells lacking Sty1, some genes were still up-regulated upon heat shock, and those were supposed to be Hsf1 dependent (Chen et al., 2003). Figure 3A shows a cluster analysis of 218 genes up-regulated more than 2-fold in basal conditions in a *Δmas5* strain (first track) (Vjestica et al., 2013), compared with the fold induction of those genes upon heat shock at 39°C in either a wild-type background (second track) or in cells lacking Sty1 (third track) (Chen et al., 2003). The transcriptome of untreated *Δmas5* strain displays some genes that are up-regulated with respect to untreated wild-type cells, and that are triggered upon heat shock in a Sty1-dependent and independent manner (Figure 3A). In fact, out of the 218 genes up-regulated more than 2-fold in cells lacking Mas5, one-third are up-regulated upon heat shock in both a wild-type and a *Δsty1* background, whereas another third are Sty1-dependent heat shock-inducible genes (Figure 3B).

To confirm that cells lacking Mas5 display up-regulation not only of Hsf1-dependent genes but also of Sty1-Atf1 genes, we compared the up-regulated transcriptome of strain *Δmas5* with that of cells expressing the constitutively active Atf1.10D mutant (Salat-Canela et al., 2017). As shown in Figures 3C and 3D, 48 of 218 genes up-regulated more than 2-fold in cells lacking Mas5 are up-regulated more than 2-fold in the absence of stress in cells expressing Atf1.10D.

As the three datasets compared above were obtained with different experimental and technical conditions (Chen et al., 2003; Salat-Canela et al., 2017; Vjestica et al., 2013), we decided to provide further support to the idea that cells lacking Mas5 display two up-regulated gene expression programs driven by the transcription factors Hsf1 and Atf1. To that end, we compared selected gene targets by northern blot in cells lacking Mas5, Atf1, or both proteins. As shown in Figure S3A, the Hsf1-dependent genes *hsp16* and *hsp104* are up-regulated in cells lacking Mas5 in an Atf1-independent manner. On the contrary, the *ctt1* and *hsp9* genes, whose expression is totally (*hsp9*) or partially (*ctt1*) dependent on Atf1, are expressed even in the absence of stress in *Δmas5* cells, and this up-regulation is abolished in *Δmas5 Δatf1* cells.

In wild-type cells, treatment with environmental stressors such as H_2O_2 triggers phosphorylation of the MAP kinase Sty1 and its downstream transcription factor Atf1. Basal phosphorylation of Sty1 and Atf1 are detected in cells lacking Mas5 (Figure 3E). Furthermore, Atf1 protein levels are also enhanced, because the *atf1* gene is subjected to a positive feedback loop (Figure 3E) (Chen et al., 2008). The peroxiredoxin Tpx1, which dimerizes during H_2O_2 scavenging, is inactivated by high concentrations of peroxides; thus dimer formation cannot be detected upon 1 mM H_2O_2 stress in extracts from wild-type cells, but it can in extracts from strain *Δmas5*, indicating that peroxides are actively being scavenged in this background (Figure 3E). We confirmed by quantitative PCR that the expression of several stress genes is

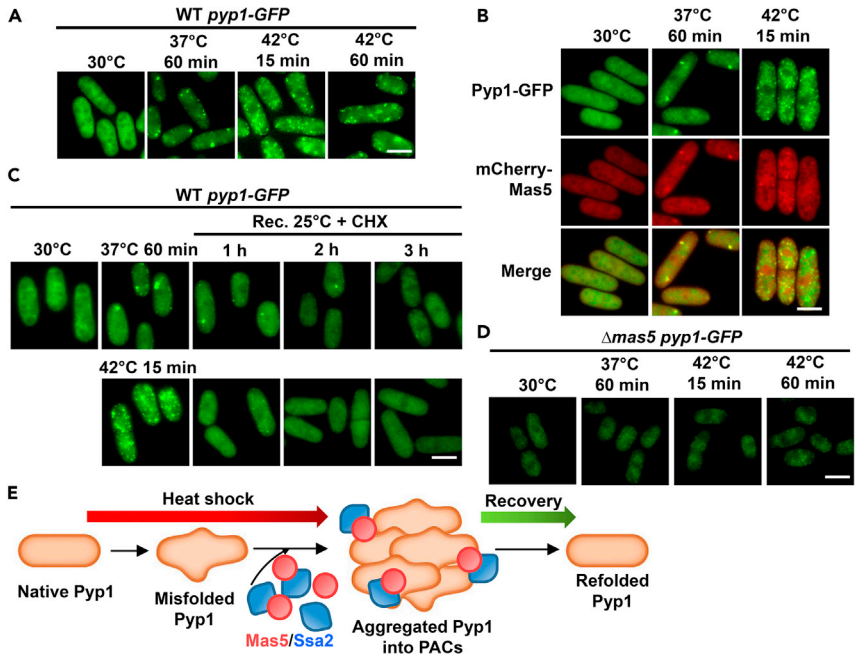

Figure 4. The Pyp1 Phosphatase Collapses into PACs Upon Heat Shock in a Mas5-Dependent Manner

(A) Pyp1 assembles into PACs upon heat stress. Formation of PACs was monitored by fluorescence microscopy in strain SB585 (expressing Pyp1-GFP) at the indicated time points and heat shock conditions. Maximum-intensity projections of z stacks (6 planes, 0.3-μm steps) are shown.

(B) Pyp1-GFP and mCherry-Mas5 co-localize in PACs upon heat shock. Strain SB642 (expressing Pyp1-GFP and mCherry-Mas5) was analyzed as in (A) at 30°C or after heat shock. Maximum-intensity projections of z stacks (6 planes, 0.3 μm steps) are shown for Pyp1-GFP.

(C) Assembled Pyp1 aggregates at 37°C or 42°C are dissolved during recovery at physiological temperature. Strain SB585 (expressing Pyp1-GFP) was heat-shocked at 37°C for 1 h or 42°C for 15 min, and then incubated at 25°C in the presence of cycloheximide (CHX) to avoid new protein synthesis. Disaggregation of PACs was monitored at the indicated time points by fluorescence microscopy.

(D) Lack of Mas5 abolishes Pyp1 PAC formation. Pyp1 aggregation was monitored at the indicated time points and heat shock conditions in strain SB586 (*Δmas5* cells expressing Pyp1-GFP). Maximum-intensity projections of z stacks (6 planes, 0.3 μm steps) are shown.

(E) Scheme depicting the inactivation and re-activation of Pyp1 by PAC assembly and disassembly. Upon heat stress misfolded Pyp1 is aggregated into PACs with the assistance of the Hsp40 and Hsp70 chaperones Mas5 and Ssa2. Once temperature conditions return to normal, Pyp1 is refolded and re-activated.

Scale bar, 5 μm. See also Figures S4 and S5.

up-regulated in cells lacking Mas5 (Figure 3F). These experiments suggest that the Sty1-Atf1 cascade is partially up-regulated in the absence of stress (and more readily inducible upon peroxide addition or heat shock; Figures 3E, 3F, S3B, and S3C, respectively) in cells lacking Mas5, which may explain the stress phenotypes of strain *Δmas5* such as resistance to H_2O_2 (Figures 1D and 1E) or elongated lifespan (Figure 3G).

The Pyp1 Phosphatase, a Negative Regulator of Sty1, Collapses into PACs upon Heat Shock in a Mas5-Dependent Manner

All the observed phenotypes of strain *Δmas5,* including longer lifespan during chronological aging, resemble those of strain *Δpyp1* (Figure 3G) (Zuin et al., 2010). In fact, cells lacking both Mas5 and Pyp1 have basal and stress-dependent phenotypes very similar to those of strain *Δmas5,* suggesting that both proteins are likely in the same pathway regarding Sty1 regulation (Figure S3D). As described above, Pyp1 is the main tyrosine phosphatase of the stress kinase Sty1, and heat shock was proposed to inhibit the interaction of Sty1 with Pyp1, leading to Sty1 activation (Nguyen and Shiozaki, 1999). We hypothesized that Pyp1 could be a thermo-unstable protein, so that heat shock imposition would largely affect the equilibrium between its native and misfolded conformation. We tagged Pyp1 with GFP, confirmed that the protein retained functionality (Figure S4A), and analyzed its subcellular localization by fluorescence microscopy.

Pyp1-GFP displays cytoplasmic localization when cells are grown at 30°C, but coalescences into fluorescent foci when cells are subjected to 37°C or 42°C stress (Figure 4A). The phosphatase does not form these foci upon H_2O_2 treatment (Figure S4B). To confirm that Pyp1 assembles into PACs together with other thermosensitive proteins and chaperones (Cabrera et al., 2020), we simultaneously expressed Pyp1-GFP and the Hsp40 mCherry-Mas5: both proteins display an almost complete co-localization upon heat stress (Figure 4B). As described before for other misfolding reporters at PACs, Pyp1-GFP is neither terminally misfolded nor destined to degradation: it can acquire soluble cytoplasmic localization during recovery at non-stressful temperatures (Figure 4C). As reported for PACs, formation of Pyp1-GFP foci during 37°C or 42°C stress is fully or partially inhibited, respectively, by cycloheximide, whereas puromycin does not impair PAC assembly (Figure S4C). Finally, an important feature of PAC formation is that it is mediated by the Hsp40/Hsp70 couple Mas5/Ssa2 (Cabrera et al., 2020). As shown in Figure 4D, Pyp1-GFP is not able to assemble into PACs in cells lacking Mas5, even if Pyp1 is over-expressed (Figure S4D). Importantly, Sty1-GFP does not aggregate into PACs upon heat shock or oxidative stress, but rather accumulates in the nucleus as previously described (Figures S5A and S5B). We conclude that heat shock-dependent Pyp1-GFP foci and PACs are the same entities, which temporarily separate Pyp1 from Sty1 (Figure 4E).

Based on the fluorescence microscopy experiments described above, Pyp1 seems to be a thermo-unstable protein that misfolds upon heat shock. To confirm it, we compared the solubility of Pyp1-GFP at permissive and restrictive temperatures. We obtained total protein extracts of Pyp1-GFP-expressing cells grown at different temperatures and isolated the soluble and pellet fractions by high-speed centrifugation, following the presence of Pyp1-GFP by western blot (Figure 5A). Pyp1-GFP was found predominantly in the soluble form at 30°C (S in Figure 5B), whereas the protein was highly enriched in the detergent-insoluble fraction of extracts from cells grown at 37°C or 42°C (P in Figure 5B). We recently performed a similar experiment from wild-type cells expressing endogenous Pyp1, and analyzed the insoluble pellet fractions with untagged liquid chromatography coupled with tandem mass spectrometry (Figure 5A) (Cabrera et al., 2020). It was observed that 160 proteins were only present in the pellet fractions of extracts from cells grown at 37°C and 42°C but not at 30°C (Cabrera et al., 2020). As shown in Figure 5C, they were classified into different Gene Ontology categories using the web-based analysis resource Metascape (Zhou et al., 2019); importantly, Pyp1 is one of the proteins identified in this proteome-wide study as part of the thermally sensitive fission yeast proteome (in red in Figure 5C).

Over-expression of Pyp1 Suppresses the H_2O_2 Resistance Phenotype of Cells Lacking Mas5

We have shown above that Pyp1 has tendency to misfold during heat shock and to assemble into PACs. We wondered whether these properties could explain the increased tolerance to oxidative stress of *Δmas5* strain. As shown in Figure 6A, the concentration of Pyp1-GFP is significantly lower in cells lacking Mas5 that in wild-type cells, irrespective of the growth media conditions (in fact, basal levels of Pyp1-GFP fluorescence are also significantly affected in *Δmas5;* compare Figures 4D and 4A). The low levels of Pyp1 in cells lacking Mas5 are not caused by transcriptional down-regulation of the *pyp1* gene in *Δmas5* cells, as determined by RNA sequencing (Vjestica et al., 2013). Mas5 seems to have a role in the regulation of the basal levels of Pyp1, probably attending its folding to promote a native conformation (and therefore avoiding its degradation in the absence of heat stress). Indeed, the concentration of Pyp1 in wild-type protein extracts barely decays 3 h after cycloheximide addition, whereas the protein almost disappears from extracts of a *Δmas5* background (Figure 6B). Furthermore, we constructed a conditional *mas5* knockout strain, in which expression of *mas5* is under the control of the thiamine-repressible *nmt41* promoter; 6 h after thiamine addition the expression of the *mas5 mRNA* is not detectable, the levels of Pyp1-GFP are reduced to those of a *Δmas5* strain (Figure S6A), and the expression of Hsf1- and Sty1-dependent genes is enhanced (Figure S6B). Mas5 also contributes during heat shock to the temporal inactivation of Pyp1 into PACs (Figures 4D and S4D); concomitantly, the phosphatase is not enriched in detergent-resistant pellet fractions of protein extracts in cells lacking Mas5 (Figure S6C).

The low steady-state levels of Pyp1 tyrosine phosphatase in strain *Δmas5* could be insufficient to maintain the Sty1 kinase inactive in the absence of stress. In response to either H_2O_2 (Figure 6C) or heat shock (Figure S3B) Sty1 is phosphorylated by its upstream kinase, Wis1, in both a serine and a tyrosine residue separated by only one amino acid (Millar et al., 1995; Shiozaki and Russell, 1995). We purified Sty1 with agarose Ni-NTA beads from extracts of wild-type or *Δmas5* cells carrying a chromosomal copy of *sty1-HA6His*, and analyzed by western blot the levels of phosphorylated tyrosine using commercial antibodies (Tyr-P in Figure 6C). Cells lacking Mas5 show enhanced levels of Sty1 phosphorylated in tyrosine in the absence of

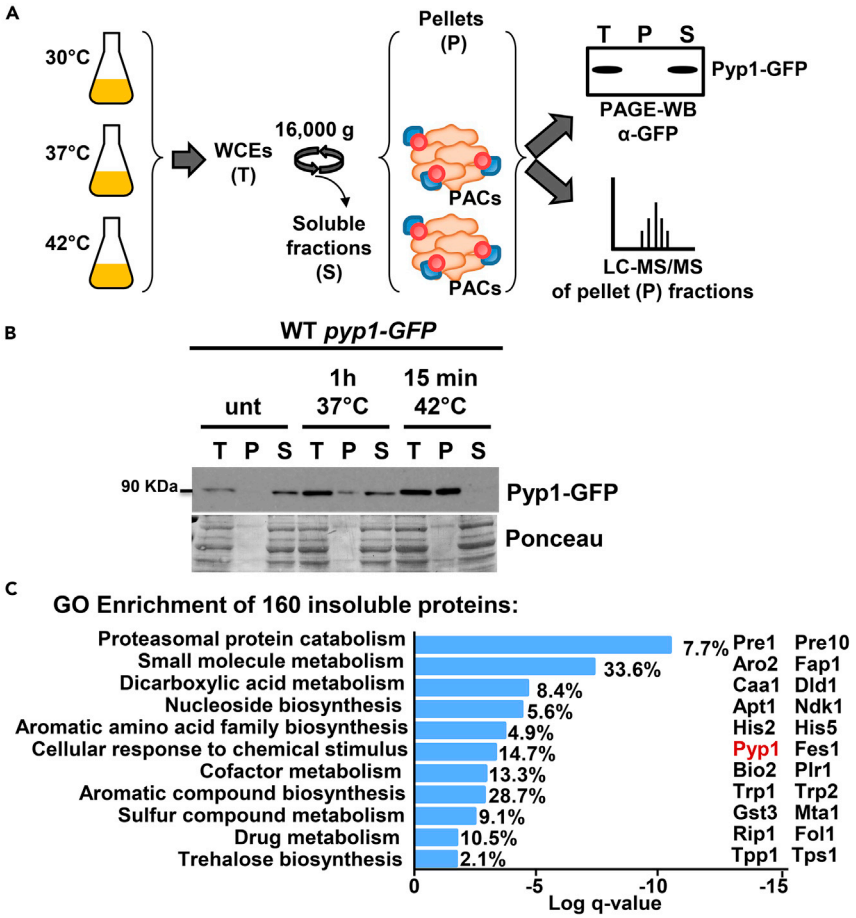

Figure 5. Pyp1 Is a Thermo-sensitive Protein

(A) Scheme depicting the experimental design to identify insoluble proteins by western blot or mass spectrometry (MS). Whole-cell extracts (WCE) from cultures grown at different temperatures (T) were centrifuged to separate insoluble pellets (P) from soluble fractions (S). Proteins enriched in the P fractions were subjected to trypsin digestion and identified by label-free liquid chromatography coupled with tandem MS (LC-MS/MS). Alternatively, the T, P and S fractions of cells expressing Pyp1-GFP were analyzed by western blot using anti-GFP antibody.

(B) Pyp1-GFP is enriched in the insoluble fraction after heat shock treatment. Solubility of Pyp1-GFP after heat shock at 37°C for 1 h and 42°C for 15 min was examined by western blot as depicted in (A). Ponceau staining was used as loading control.

(C) Gene Ontology enrichment of heat-dependent insoluble proteins. Following the scheme shown in (A) analyzed by MS, we identified 160 proteins present in the insoluble fractions of both 37°C or 42°C extracts, but not 30°C (Cabrera et al., 2020). We classify them in non-exclusive Biological process GO terms using Metascape. Each bar represents a Biological Process GO term ordered by decreasing statistical significance (Log q-value). The percentage of genes (out of 160) assigned to each GO term is shown. Two genes from each GO term are shown as examples.

stress when compared with wild-type cells (Figure 6C), suggesting that Pyp1 function is impaired in strain *Δmas5*.

We next wondered whether the *Δmas5* phenotypes (enhanced basal levels of active Sty1 and lack of accumulation of protein carbonyls upon oxidative stress) could be suppressed just by over-expressing the Pyp1 phosphatase. We expressed GFP-Pyp1 from a strong promoter in *Δmas5* cells (the functionality of the GFP-Pyp1 protein is maintained as shown in Figure S4A) and determined that the expression levels of GFP-Pyp1 are similar to those in a wild-type background (Figure 6D), the levels of basal phosphorylated Sty1 are diminished (Figure 6C), and the expression of Sty1-Atf1-dependent genes is reduced to wild-type levels (Figure S6D), whereas the Hsf1-dependent genes remain high (Figure S6E). Most importantly, expression of Pyp1 from the strong promoter was sufficient to suppress the lack of accumulation of protein carbonyls in

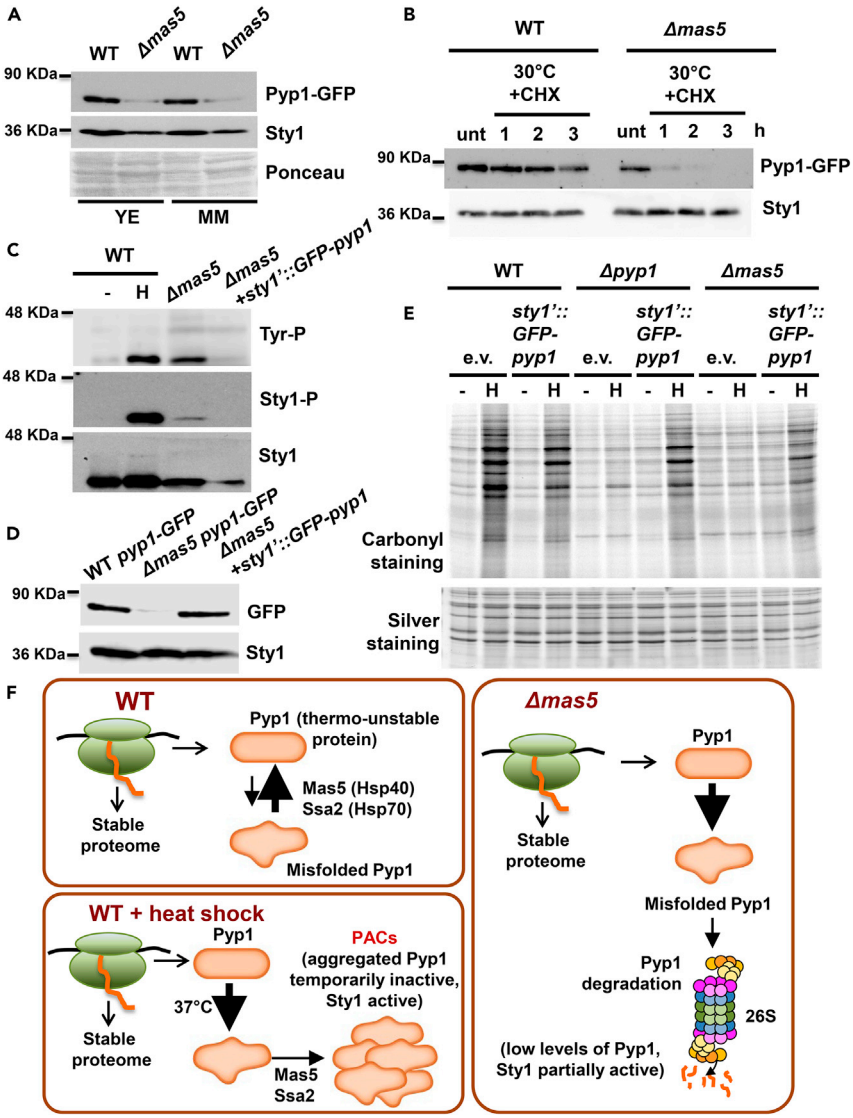

Figure 6. Pyp1 Activity Is Compromised in Cells Lacking Mas5

(A) Pyp1 levels are decreased in cells lacking Mas5. Pyp1-GFP levels were analyzed by western blot from total TCA extracts of SB585 (WT) and SB586 (*Δmas5*) cells grown in YE or MM. Sty1 and Ponceau staining are used as loading controls.

(B) Pyp1-GFP is less stable in cells lacking Mas5. Strain SB585, expressing Pyp1-GFP, and strain SB586, expressing Pyp1-GFP and lacking Mas5, were treated with cycloheximide (CHX) for the indicated times and Pyp1-GFP levels were determined by western blot from TCA extracts. Sty1 is used as loading control.

(C) Pyp1 activity is decreased in cells lacking Mas5. Sty1 was purified by Ni-NTA agarose beads from strains SB584 (*Δmas5 sty1-HA6His*) and SB649 (*Δmas5 sty1-HA6His sty1'::GFP-pyp1*), both carrying a chromosomal copy of *sty1* tagged with *HA6His* and the second expressing GFP-Pyp1 from the strong *sty1* promoter. Immuno-precipitates were subjected to western blot analysis with anti-phosphotyrosine (Tyr-P), anti-phospho-p38 (Sty1-P), and anti-Sty1 antibodies. Immuno-precipitates from strain JA578 (WT *sty1-HA6His*), treated or not with 1 mM H_2O_2 for 15 min (H), was used as a control.

(D) Overexpression of GFP-Pyp1 in cells lacking Mas5 restores wild-type levels of Pyp1. Levels of GFP-Pyp1 were examined by western blot using GFP antibody in native protein extracts from SB585 (WT), SB586 (*Δmas5*), both bearing a chromosomal copy of *pyp1-GFP*, and SB605 (*Δmas5* cells carrying a copy of an integrative plasmid expressing GFP-Pyp1 under the control of the *sty1* promoter).

(E) Overexpression of GFP-Pyp1 in cells lacking Mas5 restores protein carbonyl formation upon oxidative stress. Protein carbonyls were analyzed in SB472 (WT), SB597 (*Δpyp1*), and SB598 (*Δmas5*) cells carrying a copy of an integrative empty vector (e.v.) or in SB589 (WT), SB592 (*Δpyp1*), and SB605 (*Δmas5*) cells carrying a copy of an integrative plasmid expressing GFP-Pyp1 under the control of the *sty1'* promoter and treated with 2.5 mM H_2O_2 for 4 h (H). Silver staining is used as loading control.

Figure 6. *Continued*
(F) Model depicting the role of the Hsp40 chaperone Mas5 in PQC and in the regulation of the Sty1-dependent general stress response. WT (upper panel): during permissive temperatures, the Mas5/Ssa2 chaperones are required to assist refolding of aggregation-prone proteins such as Pyp1. WT + heat shock (lower panel): upon heat stress, general protein misfolding probably overwhelms the folding capacity of Mas5/Ssa2, and these chaperones promote PAC formation including Pyp1, which is temporally sequestered releasing and activating Sty1. *Δmas5* (right panel): in the absence of Mas5, misfolded Pyp1 accumulates, PACs cannot be formed, and the phosphatase is no longer protected from degradation by the 26S proteasome, leaving Sty1 unattended and active in the absence of stress.
See also Figure S6.

extracts from *Δmas5* cells (Figure 6E). We conclude that cells lacking Mas5 display reduced levels of Pyp1, high levels of active Sty1, and concomitantly enhanced tolerance to oxidative stress.

DISCUSSION

Within a given proteome, some proteins have more tendency to misfold than others, and therefore require to a larger extent the active participation of the PQC system even in the absence of stress signals. We propose that the Pyp1 phosphatase is one of such proteins, and that the Hsp40/70 Mas5/Ssa2 couple actively catalyzes its misfolded-to-native structure conformation, and therefore avoids Pyp1 degradation. The fact that cells lacking the chaperone Mas5 express low levels of Pyp1 supports the idea that Pyp1 has tendency to misfold. In wild-type cells, this tendency is crucial for Pyp1 activity, because the phosphatase actively maintains the stress kinase Sty1 inactive in the absence of stress, but it is temporarily sequestered into PACs upon heat shock to allow full activation of Sty1. Our experiments suggest that Pyp1 is a thermo-sensitive protein that reversibly regulates the activity of the MAP kinase Sty1 specifically upon heat shock (Figure 6F).

By characterizing the enhanced tolerance to oxidative stress of strain *Δmas5*, we have demonstrated that this Hsp40 chaperone, together with the Hsp70 Ssa2, has important roles not only upon heat shock but also during basal conditions. During growth in the absence of environmental stressors, we propose that Mas5 interacts with non-native proteins with enhanced tendency to aggregate, such as Pyp1, and participates in their refolding. Upon heat shock, where misfolded clients overwhelm the folding capacity of Mas5/Ssa2, the chaperone participates in the following: (1) it promotes the aggregation of non-terminally misfolded clients into PACs to prevent their degradation (Cabrera et al., 2020); (2) by temporally sequestering Pyp1 into PACs, it triggers the transient activation of Sty1 and the core environmental stress response, and (3) it releases the transcription factor Hsf1 to up-regulate its downstream genes (Vjestica et al., 2013). We propose that Mas5 is a master regulator connecting the PQC system with the Sty1-dependent general stress response system in *S. pombe*.

In a previous study, we identified by mass spectrometry the thermo-unstable proteome of *S. pombe* by comparing the detergent-insoluble fraction of extracts from 30°C, 37°C, and 42°C (Figure 5A) (Cabrera et al., 2020). Thus, 210 endogenous proteins were enriched in the insoluble fractions of 37°C and 42°C, from which 160 were not even present in the pellets of cells grown at 30°C (Cabrera et al., 2020). We demonstrate now that the coalescence into PACs of one of them, Pyp1, has a biological role, the activation of the general stress response driven by Sty1. We are currently investigating whether other proteins identified in our studies are also temporarily inactivated into these aggregation-like foci with a purpose, such as the metabolic re-programming proposed for Cdc19 in budding yeast (Saad et al., 2017). We propose that protein coalescence into PACs may not only protect misfolded proteins from degradation but also constitute a post-translational regulatory on-off switch of protein activity.

In budding yeast, the Mas5 homolog Ydj1 has been proposed, among other functions, to protect nascent protein kinases from degradation (Mandal et al., 2008), to control the stoichiometry of the transcription and repair factor TFIIH (Moriel-Carretero et al., 2011), and to promote during heat shock, together with the E3 ligase Rsp5, the degradation of misfolded substrates (Fang et al., 2014). Therefore, this Hsp40 in *S. cerevisiae* also has a plethora of functions during both basal and stress conditions. We propose that Mas5, Ydj1, and their homologs in other eukaryotic organisms control the transition from basal proteostasis to the heat-induced up-regulation of the PQC system.

Limitations of the Study

In this study, we have uncovered three associated (but distinct) functions of the Hsp40 Mas5. First, at permissive temperature, the Hsp40/70 Mas5/Ssa2 couple actively catalyzes refolding of all the proteins

that have high tendency to misfold, such as the phosphatase Pyp1 (inhibitor of the MAP kinase Sty1), and, therefore, prevents Pyp1 degradation. It is still formally possible, that decreased Pyp1 levels in cells lacking Mas5 could be attributable to a general decrease in total protein, due, for instance, to non-optimal protein translation. However, proteomic data from cells lacking Mas5 indicate that only a small subset of proteins has lower levels than wild-type. It will be interesting to identify E3 ligases whose deficiency restores wild-type Pyp1 levels in basal conditions in a *Δmas5* background. Second, during heat shock, Mas5/Ssa2 facilitates the coalescence of all the unstable proteome into PACs. In the case of Pyp1, this causes its transient inactivation, and the secondary activation of the Sty1 stress program. Mas5 co-localizes with Pyp1 upon heat shock suggesting an interaction in these conditions, and we propose that Mas5 interacts with Pyp1 also in basal conditions. However, it is experimentally difficult to biochemically (e.g., co-IP) demonstrate an interaction between folding chaperones, such as Mas5/Ssa2, and their substrates in basal conditions due to the transient nature of the interaction, and such a demonstration is missing. Nonetheless, the plethora of roles assigned to the Mas5 homolog in budding yeast, Ydj1, like protecting nascent protein kinases from degradation strengthens the notion that Mas5 physically interacts with Pyp1. Finally, at permissive temperature, the couple Hsp40/70 Mas5/Ssa2 inhibits two heat shock-dependent gene expression programs: the well-studied Hsf1-dependent program and the one driven by the MAP kinase Sty1. This suggests the idea that there can be a cross talk between these two relevant pathways that can be further explored in fission yeast and other model systems.

Resource Availability

Lead Contact

Further information and requests for resources and reagents should be directed to and will be fulfilled by the Lead Contact, Elena Hidalgo (elena.hidalgo@upf.edu).

Materials Availability

This study did not generate new unique reagents.

Data and Code Availability

All images included in the main and supplemental figures are available as Mendeley dataset (https://doi.org/10.17632/zwkh97bdw9.1).

METHODS

All methods can be found in the accompanying Transparent Methods supplemental file.

SUPPLEMENTAL INFORMATION

Supplemental Information can be found online at https://doi.org/10.1016/j.isci.2020.101725.

ACKNOWLEDGMENTS

We thank Snezhana Oliferenko and Miguel Rodríguez-Gabriel for providing strains and Gabriel Gil for kindly providing antibodies against phospho tyrosine. This work is supported by the Ministerio de Ciencia, Innovación y Universidades, PLAN E and FEDER (Spain) (PGC2018-093920-B-I00 to E.H.). The Oxidative Stress and Cell Cycle group is also supported by Generalitat de Catalunya (Spain) (2017-SGR-539) and by Unidad de Excelencia María de Maeztu, funded by the AEI (Spain) (CEX2018-000792-M). M.C. is funded by the Ramon y Cajal program (Spain) (MINECO-RYC2013-12858). E.H. is recipient of an ICREA Academia Award (Generalitat de Catalunya, Spain).

AUTHOR CONTRIBUTIONS

S.B. and L.M. performed most experiments. S.B., L.M., S. G.-S., M.V., M.C., J.A., and E.H. analyzed the data. E.H. wrote the manuscript.

DECLARATION OF INTERESTS

The authors declare no competing interests.

Received: May 6, 2020
Revised: August 3, 2020
Accepted: October 20, 2020
Published: November 20, 2020

REFERENCES

Cabrera, M., Boronat, S., Marte, L., Vega, M., Perez, P., Ayte, J., and Hidalgo, E. (2020). Chaperone-facilitated aggregation of thermo-sensitive proteins shields them from degradation during heat stress. Cell Rep. *30*, 2430–2443.e4.

Craig, E.A., and Marszalek, J. (2017). How do J-proteins get Hsp70 to do so many different things? Trends Biochem. Sci. *42*, 355–368.

Chen, D., Toone, W.M., Mata, J., Lyne, R., Burns, G., Kivinen, K., Brazma, A., Jones, N., and Bahler, J. (2003). Global transcriptional responses of fission yeast to environmental stress. Mol. Biol. Cell *14*, 214–229.

Chen, D., Wilkinson, C.R., Watt, S., Penkett, C.J., Toone, W.M., Jones, N., and Bahler, J. (2008). Multiple pathways differentially regulate global oxidative stress responses in fission yeast. Mol. Biol. Cell *19*, 308–317.

Escusa-Toret, S., Vonk, W.I.M., and Frydman, J. (2013). Spatial sequestration of misfolded proteins by a dynamic chaperone pathway enhances cellular fitness during stress. Nat. Cell Biol. *15*, 1231.

Fang, N.N., Chan, G.T., Zhu, M., Comyn, S.A., Persaud, A., Deshaies, R.J., Rotin, D., Gsponer, J., and Mayor, T. (2014). Rsp5/Nedd4 is the main ubiquitin ligase that targets cytosolic misfolded proteins following heat stress. Nat. Cell Biol. *16*, 1227–1237.

Hipp, M.S., Kasturi, P., and Hartl, F.U. (2019). The proteostasis network and its decline in ageing. Nat. Rev. Mol. Cell Biol. *20*, 421–435.

Jayaraj, G.G., Hipp, M.S., and Hartl, F.U. (2020). Functional modules of the proteostasis network. Cold Spring Harb. Perspect. Biol. *12*, a033951.

Kampinga, H.H., and Craig, E.A. (2010). The HSP70 chaperone machinery: J proteins as drivers of functional specificity. Nat. Rev. Mol. Cell Biol. *11*, 579–592.

Kim, K.D., Chung, W.H., Kim, H.J., Lee, K.C., and Roe, J.H. (2010). Monothiol glutaredoxin Grx5 interacts with Fe-S scaffold proteins Isa1 and Isa2 and supports Fe-S assembly and DNA integrity in mitochondria of fission yeast. Biochem. Biophys. Res. Commun. *392*, 467–472.

Kim, Y.E., Hipp, M.S., Bracher, A., Hayer-Hartl, M., and Hartl, F.U. (2013). Molecular chaperone functions in protein folding and proteostasis. Annu. Rev. Biochem. *82*, 323–355.

Kominek, J., Marszalek, J., Neuveglise, C., Craig, E.A., and Williams, B.L. (2013). The complex evolutionary dynamics of Hsp70s: a genomic and functional perspective. Genome Biol. Evol. *5*, 2460–2477.

Liu, Q., Liang, C., and Zhou, L. (2020). Structural and functional analysis of the Hsp70/Hsp40 chaperone system. Protein Sci. *29*, 378–390.

Mandal, A.K., Nillegoda, N.B., Chen, J.A., and Caplan, A.J. (2008). Ydj1 protects nascent protein kinases from degradation and controls the rate of their maturation. Mol. Cell. Biol. *28*, 4434–4444.

Marte, L., Boronat, S., Garcia-Santamarina, S., Ayte, J., Kitamura, K., and Hidalgo, E. (2020). Identification of ubiquitin-proteasome system components affecting the degradation of the transcription factor Pap1. Redox Biol. *28*, 101305.

Millar, J.B., Buck, V., and Wilkinson, M.G. (1995). Pyp1 and Pyp2 PTPases dephosphorylate an osmosensing MAP kinase controlling cell size at division in fission yeast. Genes Dev. *9*, 2117–2130.

Miller, S.B., Ho, C.T., Winkler, J., Khokhrina, M., Neuner, A., Mohamed, M.Y., Guilbride, D.L., Richter, K., Lisby, M., Schiebel, E., et al. (2015). Compartment-specific aggregases direct distinct nuclear and cytoplasmic aggregate deposition. EMBO J. *34*, 778–797.

Moriel-Carretero, M., Tous, C., and Aguilera, A. (2011). Control of the function of the transcription and repair factor TFIIH by the action of the cochaperone Ydj1. Proc. Natl. Acad. Sci. U S A *108*, 15300–15305.

Nguyen, A.N., and Shiozaki, K. (1999). Heat-shock-induced activation of stress MAP kinase is regulated by threonine- and tyrosine-specific phosphatases. Genes Dev. *13*, 1653–1663.

Okazaki, K., Kato, H., Iida, T., Shinmyozu, K., Nakayama, J.I., Murakami, Y., and Urano, T. (2018). RNAi-dependent heterochromatin assembly in fission yeast Schizosaccharomyces pombe requires heat-shock molecular chaperones Hsp90 and Mas5. Epigenetics Chromatin *11*, 26.

Pilla, E., Schneider, K., and Bertolotti, A. (2017). Coping with protein quality control failure. Annu. Rev. Cel. Dev. Biol. *33*, 439–465.

Saad, S., Cereghetti, G., Feng, Y., Picotti, P., Peter, M., and Dechant, R. (2017). Reversible protein aggregation is a protective mechanism to ensure cell cycle restart after stress. Nat. Cell Biol. *19*, 1202–1213.

Salat-Canela, C., Paulo, E., Sanchez-Mir, L., Carmona, M., Ayte, J., Oliva, B., and Hidalgo, E. (2017). Deciphering the role of the signal- and Sty1 kinase-dependent phosphorylation of the stress-responsive transcription factor Atf1 on gene activation. J. Biol. Chem. *292*, 13635–13644.

Shiozaki, K., and Russell, P. (1995). Cell-cycle control linked to extracellular environment by MAP kinase pathway in fission yeast. Nature *378*, 739–743.

Sontag, E.M., Samant, R.S., and Frydman, J. (2017). Mechanisms and functions of spatial protein quality control. Annu. Rev. Biochem. *86*, 97–122.

Vjestica, A., Zhang, D., Liu, J., and Oliferenko, S. (2013). Hsp70-Hsp40 chaperone complex functions in controlling polarized growth by repressing Hsf1-driven heat stress-associated transcription. PLoS Genet. *9*, e1003886.

Wilkinson, M.G., Samuels, M., Takeda, T., Toone, W.M., Shieh, J.C., Toda, T., Millar, J.B., and Jones, N. (1996). The Atf1 transcription factor is a target for the Sty1 stress-activated MAP kinase pathway in fission yeast. Genes Dev. *10*, 2289–2301.

Zhou, Y., Zhou, B., Pache, L., Chang, M., Khodabakhshi, A.H., Tanaseichuk, O., Benner, C., and Chanda, S.K. (2019). Metascape provides a biologist-oriented resource for the analysis of systems-level datasets. Nat. Commun. *10*, 1523.

Zuin, A., Carmona, M., Morales-Ivorra, I., Gabrielli, N., Vivancos, A.P., Ayte, J., and Hidalgo, E. (2010). Lifespan extension by calorie restriction relies on the Sty1 MAP kinase stress pathway. Embo J. *29*, 981–991.

iScience, Volume *23*

Supplemental Information

The Hsp40 Mas5 Connects Protein Quality Control and the General Stress Response through the Thermo-sensitive Pyp1

Susanna Boronat, Luis Marte, Montserrat Vega, Sarela García-Santamarina, Margarita Cabrera, José Ayté, and Elena Hidalgo

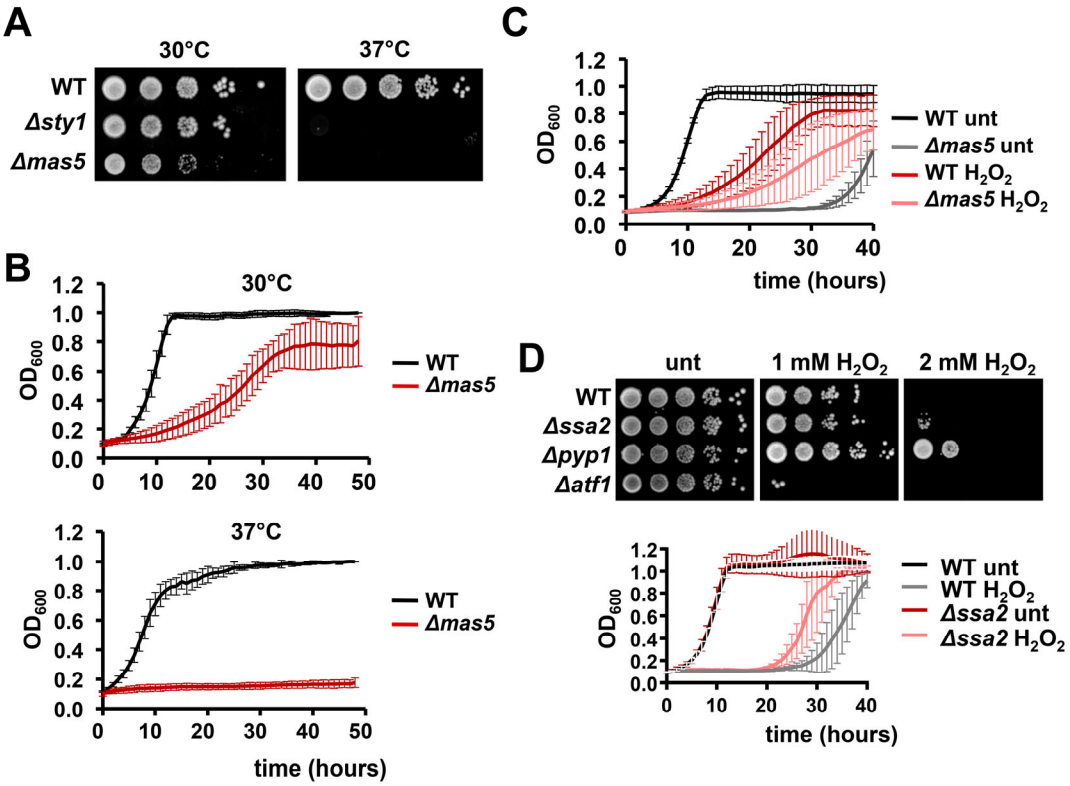

Figure S1. Cells lacking Mas5 are sensitive to heat stress, but not to H_2O_2 (Related to Figure 1).
(A) Cells lacking Mas5 do not grow at 37°C. Serial dilutions of strains 972 (WT), AV18 (*Δsty1*, used as a heat shock–sensitive control strain) and SB26 (*Δmas5*) were spotted on YE plates and incubated at 30°C or 37°C for three days.
(B) Growth of liquid cultures of strains 972 (WT) and SB26 (*Δmas5*) at 30°C and 37°C was monitored by reading the OD_{600} during 48 hours. Data representing the average of three independent experiments with error bars (S.D.) are shown.
(C) Growth of 972 (WT) and SB26 (*Δmas5*) cells was analyzed as in Figure 1E. Data representing the average of three independent experiments with error bars (S.D.) is shown.
(D) Cells lacking Ssa2 are partially resistant to oxidative stress. Upper panel: Serial dilutions of YE cultures of strains 972 (WT), SG289 (*Δssa2*), EP48 (*Δpyp1*) and MS98 (*Δatf1*) were spotted on YE plates containing the indicated concentrations of H_2O_2 and incubated at 30°C for 2 days. Lower panel: Growth of 972 (WT) and SG289 (*Δssa2*) cells was analyzed as in Figure 1E. Data representing the average of three independent experiments with error bars (S.D.) is shown.

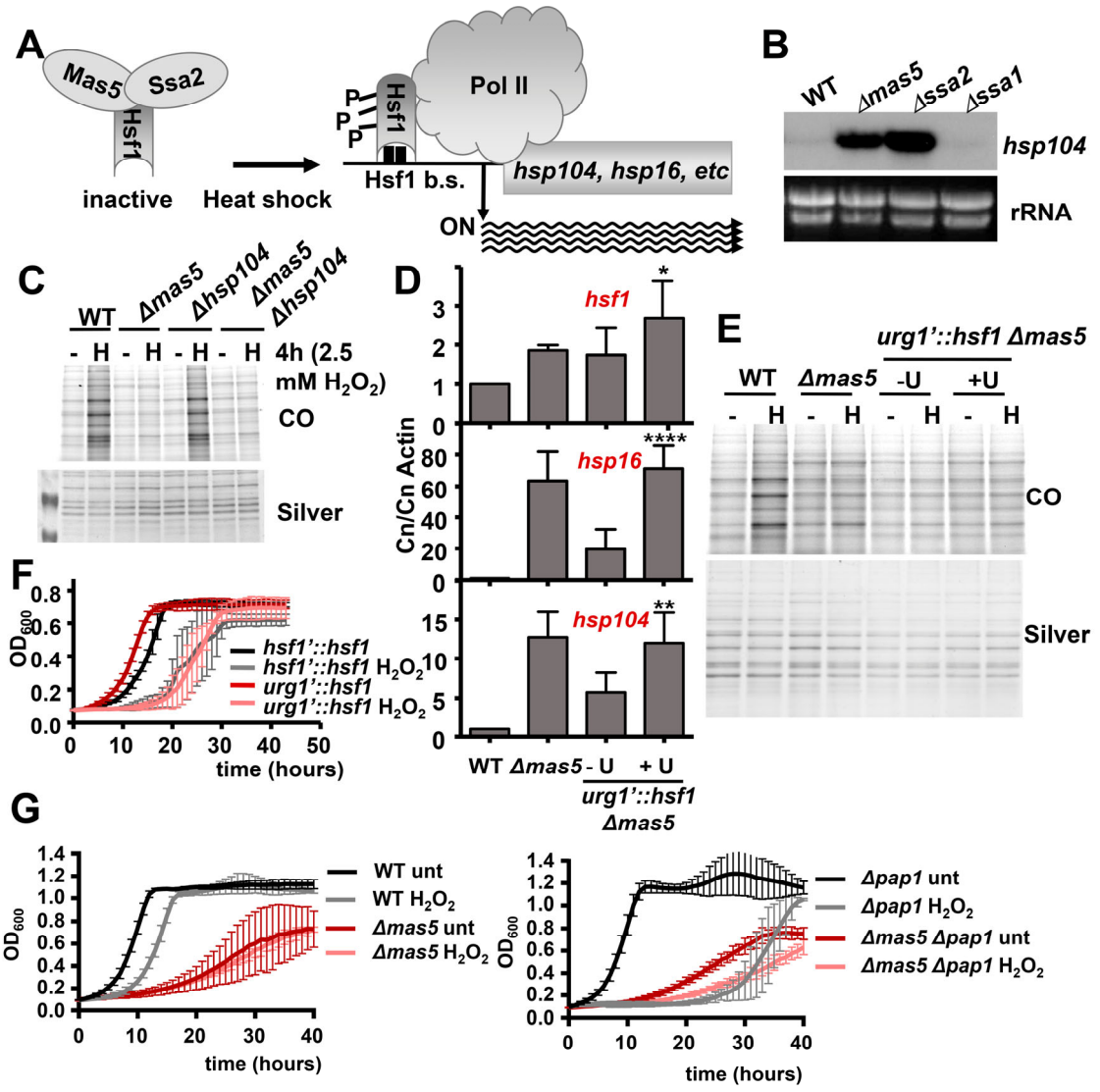

Figure S2. Constitutive activation of Hsf1 in cells lacking Mas5 does not explain the resistance to oxidative stress (Related to Figure 2).

(A) Model summarizing control of the transcription factor Hsf1 by Mas5/Ssa2. In basal conditions, Mas5/Ssa2 keeps Hsf1 inactive. Upon heat shock, Hsf1 is released, phosphorylated and binds at the Hsf1 binding sites (Hsf1 b.s.) of target genes, where it recruits RNA polymerase II (Pol II) to trigger transcription of genes such as *hsp104* and *hsp16*.

(B) Hsf1 is constitutively active in cells lacking Mas5. Northern blot showing the basal levels of *hsp104* mRNA in strains 972 (WT), SB26 (*Δmas5*), SG298 (*Δssa2*) and SB291 (*Δssa1*) grown in YE. rRNA is used as loading control.

(C) The *hsp104* gene is not a suppressor of *Δmas5*. Protein carbonyls (CO) of extracts of strains 972 (WT), SB26 (*Δmas5*), SG287 (*Δhsp104*) and SG300 (*Δmas5 Δhsp104*), treated or not with 2.5 mM H_2O_2 for 4 hours, were analyzed and quantified as in Figure 1B.

(D) Control of Hsf1 expression in *Δmas5* cells with the *urg1* promoter. The levels of *hsf1*, *hsp16* and *hsp104* mRNA were quantified by RT-qPCR in strains stains 972 (WT), SB26 (*Δmas5*) and SO7701 (*Δmas5* expressing Hsf1 under the control of the uracil-dependent *urg1* promoter), in the presence or absence or uracil during 48 hours (U). Data correspond to three biological replicates. Data is expressed as the mRNA copy number (Cn) relative to Actin Cn of each strain related to the Cn/Cn Actin of WT which is set to 1. Error bars represent S.D. Statistical significance was calculated for the indicated samples compared to WT with an unpaired t-Student test and 95% confidence level with P-values of 0.05 (*), 0.01 (**) and 0.0001 (****).

(E) Repression of *hsf1* in *Δmas5* does not restore wild-type H_2O_2-induced levels of protein carbonyls. Protein carbonyls (CO) of strains as in (D) were analyzed as in Figure 1B.
(F) Increased levels of Hsf1 in wild-type cells do not cause resistance to H_2O_2. Growth curves of strains 666 (WT, with the endogenous *hsf1* gene under the control of its own promoter, *hsf1'::hsf1*) and SB273 (carrying Hsf1 expression under the control of the *urg1* promoter (*urg1'::hsf1'*) grown in the presence of uracil, with (gray for 666 and pink for SB273) or without (black for 666 and red for SB273) 1 mM H_2O_2. Data represent the average of three independent experiments with error bars (S.D.).
(G) Cells lacking Mas5 and Pap1 display better tolerance to oxidative stress than Δ*pap1* cells. Growth of 972 (WT) and SB26 (*Δmas5*) (left panel), AV25 (*Δpap1*) and SG301 (*Δmas5 Δpap1*) (right panel) in the absence or presence of 0.5 mM H_2O_2 was monitored during 40 hours by reading the OD_{600}. Data representing the average of three independent experiments with error bars (S.D.) is shown.

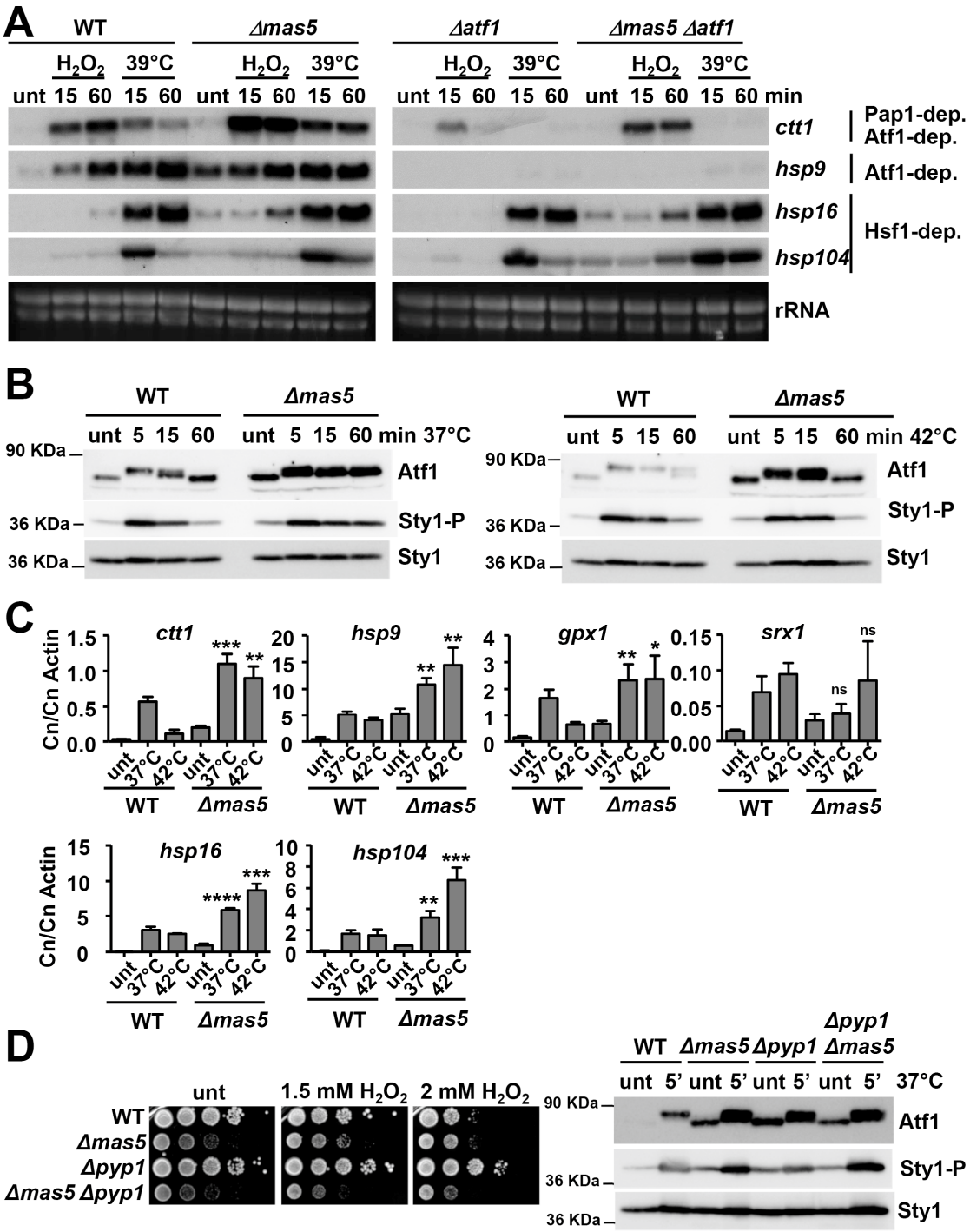

Figure S3. The stress *ctt1* and *hsp9* genes are de-repressed in cells lacking Mas5 in a Atf1-dependent manner (Related to Figure 3)

(A) The mRNA levels of Sty1-dependent (*ctt1* and *hsp9*) and Hsf1-dependent (*hsp16* and *hsp104*) genes from 972 (WT) and SB26 (*Δmas5*) cells growing in YE and treated with the indicated oxidative and heat stress conditions was analysed by Northern blot. Total ribosomal RNA (rRNA) is used as loading control.

(B) Atf1 and Sty1 phosphorylation were examined in 972 (WT) and SB26 (*Δmas5*) cells treated with the indicated heat stress conditions by western blot of TCA extracts using Atf1, phospho-p38 (Sty1-P) and Sty1 specific antibodies. Sty1 is used as loading control.

(C) The mRNA levels of Sty1-dependent (*ctt1*, *hsp9*, *gpx1* and *srx1*) and Hsf1-dependent (*hsp16* and *hsp104*) genes from 972 (WT) and SB26 (*Δmas5*) cells treated with the indicated heat stress conditions for 15 min were determined by RT-qPCR. Data are expressed as the mRNA copy number (Cn) relative to Actin Cn and represent the average of at least three biological replicates. Error bars represent S.D. Statistical significance was calculated for the indicated samples compared to unt *Δmas5* with an unpaired

t-Student test and 95% confidence level with P-values of 0.05 (*), 0.01, (**), 0.001 (***) and 0.0001 (****). ns: non significant.
(D) Pyp1 and Mas5 are in the same pathway regarding Sty1 regulation. Left panel: serial dilutions of YE cultures of strains 972 (WT), SB26 (*Δmas5*), EP48 (*Δpyp1*) and SB677 (*Δmas5 Δpyp1*) were spotted on YE plates containing the indicated concentrations of H_2O_2 and incubated at 30°C for 3 days. Right panel: Atf1 and Sty1 phosphorylation were examined in 972 (WT), SB26 (*Δmas5*), EP48 (*Δpyp1*) and SB677 (*Δmas5 Δpyp1*) cells treated with the indicated heat stress conditions by western blot of TCA extracts with the same antibodies as in (B). Sty1 is used as loading control.

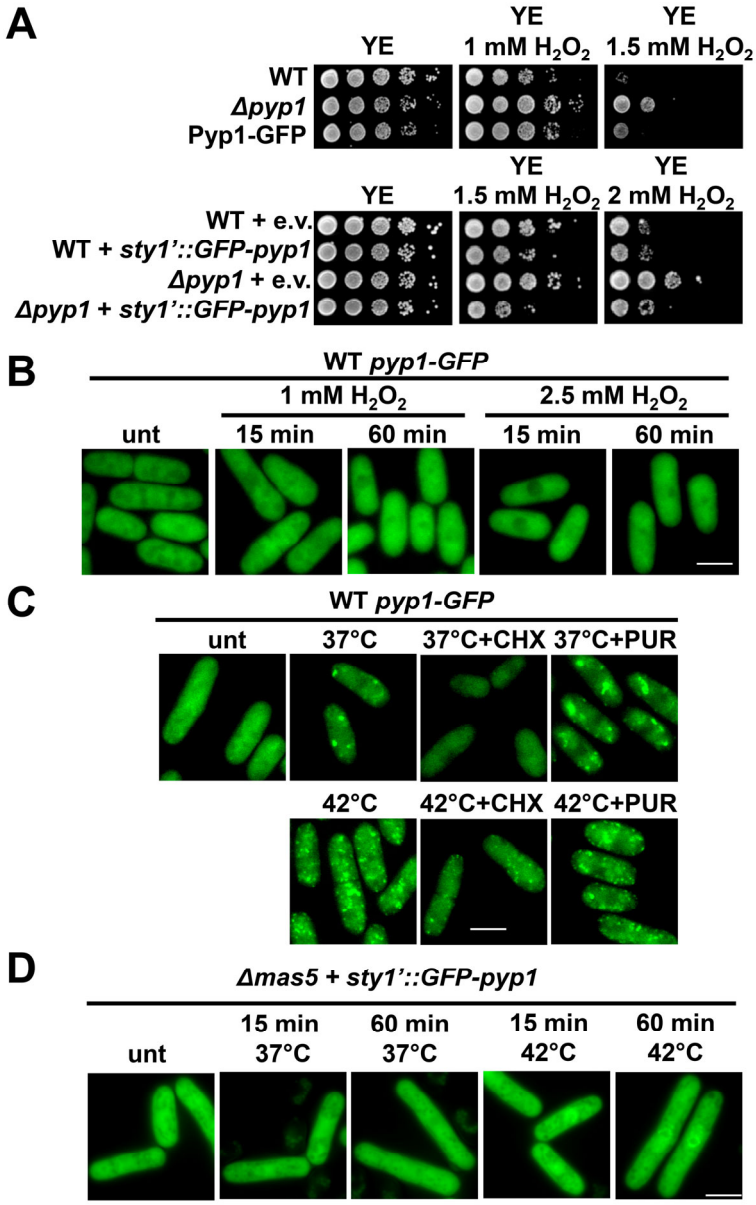

Figure S4. Pyp1-GFP aggregation into PACs (Related to Figure 4).
(A) C-terminal (upper panel) and N-terminal (lower panel) tagging of Pyp1 with GFP maintain Pyp1 functionality. Strains 972 (WT), EP48 (*Δpyp1*), and SB585 (Pyp1-GFP), harboring a *GFP* tag at the endogenous *pyp1* gene, were spotted on YE plates containing the indicated concentrations of H_2O_2 and incubated at 30°C for 3 days. Strains SB472 (WT), SB597 (*Δpyp1*) both carrying a copy of an integrative empty vector (e.v.), SB589 (WT) and SB592 (*Δpyp1*) both carrying a copy of an integrative plasmid expressing GFP-Pyp1 under the control of the constitutive *sty1* promoter were spotted on YE plates containing the indicated concentrations of H_2O_2 and incubated at 30°C for 3 days.
(B) Pyp1-GFP does not form PACs upon oxidative stress. Formation of PACs was monitored by fluorescence microscopy in strain SB585, expressing Pyp1-GFP, at the indicated oxidative stress conditions.
(C) Pyp1-GFP agregation into PACs is affected by cycloheximide (CHX) but not by puromycin (PUR). Formation of PACs was monitored by fluorescence microscopy in strain SB585, expressing Pyp1-GFP, after1 h at 37°C or 15 min at 42°C, and in the presence of 100 µg/ml CHX or 1 mM PUR. Maximum-intensity projections of z-stacks (6 planes, 0.3 µm steps) are shown. Scale bar, 5 µm.
(D) Overexpression of GFP-Pyp1 does not result in PAC formation upon heat stress in cells lacking Mas5. Formation of PACs was monitored by fluorescence microscopy in strain SB605, lacking Mas5 and expressing GFP-Pyp1 under the control of the *sty1* promoter, at the indicated heat stress conditions. Scale bar, 5 µm.

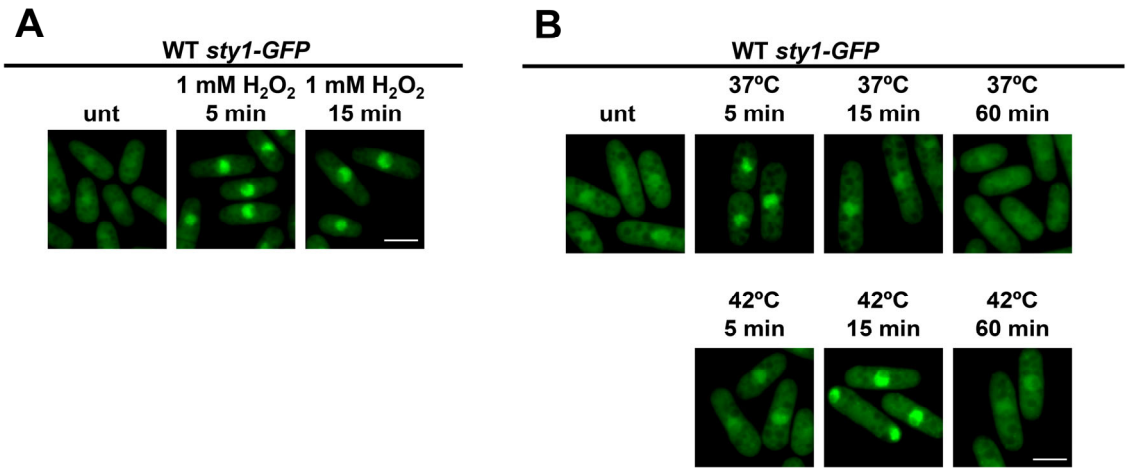

Figure S5. Sty1-GFP does not coalesce into PACs upon oxidative or heat stress (Related to Figure 4).
(A) Sty1-GFP cellular localization was monitored by fluorescence microscopy in strain EHH5, expressing Sty1-GFP, at the indicated oxidative stress conditions.
(B) Sty1-GFP cellular localization was monitored as above at the indicated heat stress conditions.
Scale bar, 5 μm.

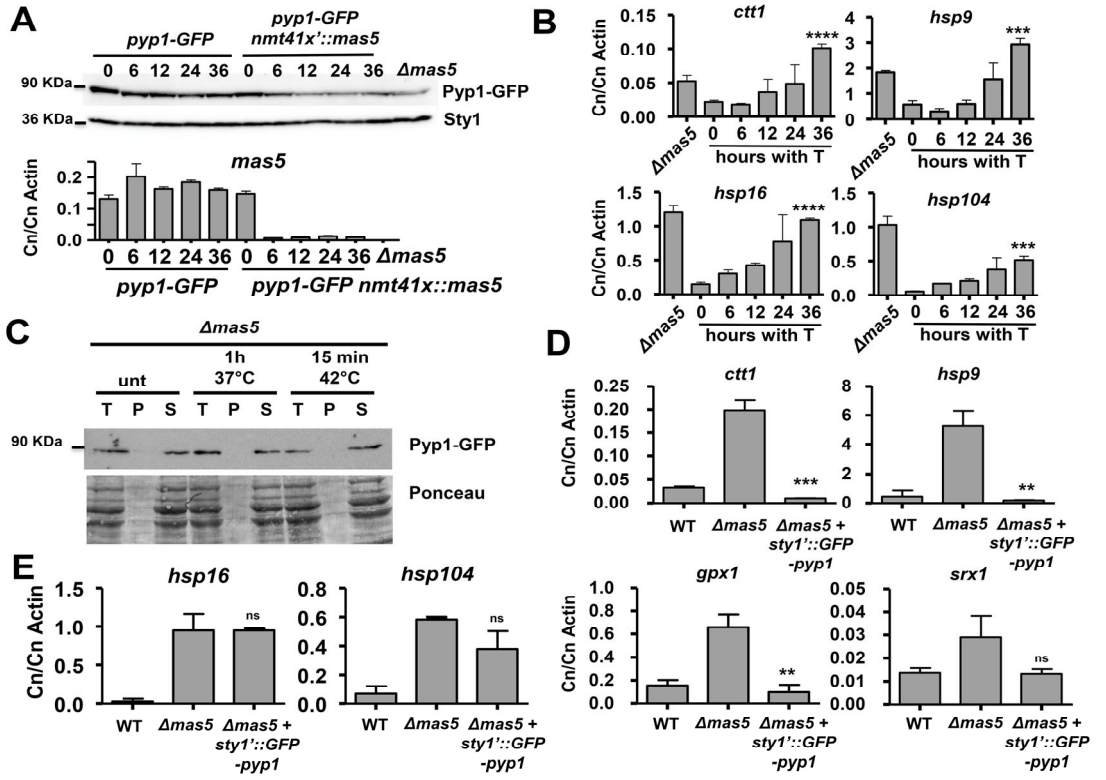

Figure S6. The concentration and activity of Pyp1 depends on Mas5 (Related to Figure 6).
(A) Pyp1-GFP levels decrease upon conditional suppression of *mas5* expression. Pyp1-GFP levels were determined by western blot from TCA extracts of strain SB678 (expressing Pyp1-GFP and carrying a copy of *mas5* under the control of the thiamine-repressible *nmt41x* promoter) grown in the absence of thiamine and left growing logarithmically for the indicated hours in the presence of thiamine. As controls, TCA extracts of strains SB585 (Pyp1-GFP) treated with the same conditions, and of untreated strain SB586 (*Δmas5* Pyp1-GFP) grown in MM, were also analyzed. Sty1 is used as loading control. To confirm thiamine-dependent *mas5* depletion, the mRNA levels of *mas5* were determined by RT-qPCR. Data are expressed as the mRNA copy number (Cn) relative to Actin Cn and represent the average of three biological replicates. Error bars represent S.D.
(B) The mRNA levels of Sty1-dependent (*ctt1* and *hsp9*) and Hsf1-dependent (*hsp16* and *hsp104*) genes from the experiment in A were determined by RT-qPCR. Data are expressed as the mRNA copy number (Cn) relative to Actin Cn and represent the average of three biological replicates. Error bars represent S.D. Statistical significance was calculated for the indicated samples compared to 0 hours with an unpaired t-Student test and 99% confidence level with P-values of 0.001 (***) and 0.0001 (****).
(C) Pyp1 does not segregate into insoluble pellets in cells lacking Mas5. Solubility of Pyp1-GFP after heat shock at 37ºC for 1 h and 42°C for 15 min was examined as in Figure 5B.
(D) Overexpression of GFP-Pyp1 suppresses increased basal levels of CESR genes of cells lacking Mas5. The mRNA levels of Sty1-dependent (*ctt1*, *hsp9*, *gpx1* and *srx1*) genes from 972 (WT), SB26 (*Δmas5*) and SB605 (*Δmas5* expressing GFP-Pyp1 under the control of the *sty1* promoter) cells logarithmically growing in YE were determined by RT-qPCR. Data are expressed as the mRNA copy number (Cn) relative to Actin Cn and represent the average of three biological replicates. Error bars represent S.D. Statistical significance was calculated for the indicated samples compared to *Δmas5* with an unpaired t-Student test and 99% confidence level with P-values of 0.01 (**) and 0.001 (***). ns: non significant
(E) Overexpression of GFP-Pyp1 does not affect the basal expression of Hsf1-dependent genes of cells lacking Mas5. The mRNA levels of Hsf1-dependent (*hsp16* and *hsp104*) genes was determined as described in D. Statistical significance was calculated for the indicated samples compared to *Δmas5* with an unpaired t-Student test and 99% confidence level. ns: non significant

TRANSPARENT METHODS

Yeast strains, plasmids and molecular biology

Yeast strains were grown in rich medium (YE) or minimal medium (MM) at 30°C as described previously (Alfa et al., 1993). The genotypes of strains used in this study are shown in Table S1. The construction of tagging of genes was done using homologous recombination with PCR fragments, using as templates pFA6a plasmid derivatives (Bahler et al., 1998). Deletion strains were obtained either by crossing deletion mutants from the Bioneer collection with wild-type strain 972 to remove auxotrophies, by homologous recombination with PCR fragments, using as templates pFA6a plasmid derivatives or, in the case of most strains lacking Mas5, by transformation with a PCR fragment obtained from genomic DNA of *mas5::kanMX6* strains encompassing approximately 500 bp upstream and downstream of the *kanMX6* cassette. Strain JA578 was derived from strain KS2088, kindly provided by M.A Rodriguez and K. Shiozaki, by crossing KS2088 with PN743 (*h^+ ade6-704 leu1-32)* from our lab stock. Integrative plasmids p669' and p705' were constructed to express N-terminally GFP-tagged Pyp1 and N-terminally mCherry-tagged Mas5, respectively, both under the control of the constitutive *sty1* promoter (Fernandez-Vazquez et al., 2013). To construct strains expressing these tagged proteins, plasmids p669' and p705' were linearized with restriction enzyme *Nru*I and integrated by recombination at the *leu1-32* allele of recipient strains. To construct strains with an empty vector, the integrative plasmid AY024 bearing the *nmt41* promoter was digested with *Nru*I and used as above. To construct strain SB678, the integrative plasmid p524.41x', expressing *mas5* under the control of the *nmt41x* promoter, was linearized as above and used to transform strain SB586.

Growth curves

OD_{600} was recorded during 48 h for cells growing in YE (unless otherwise specified) at 30ºC or 37ºC from an initial OD_{600} of 0.1 using an automated measurement as previously described (Calvo et al., 2009). When indicated, H_2O_2 was present in the cultures.

Spot assay for determination of H_2O_2 and heat shock sensitivity or chronological aging

For stress sensitivity, cells were grown in YE to logarithmic phase (OD_{600} 0.5), concentrated to OD_{600} 2.5, and 1/10 serial dilutions (from 10 to 10^5 cells) in 3 µl were spotted onto plates of rich media with or without different concentrations of H_2O_2. Plates were incubated at 30°C for 2 to 4 days. For chronological aging, cells were grown in YE to logarithmic cultures, and 3, 5 and 10 days after reaching stationary phase, and several dilutions were prepared as above and spotted onto YE plates. Plates were imaged after three days of growth at 30°C for 2 to up to 5 days (for chronological aging) or after three days of growth at 30ºC or 37°C (for heat shock stress).

Drug treatments

Cells were incubated with 0.1 mg/ml cycloheximide (Sigma-Aldrich) or 1 mM puromycin (Sigma-Aldrich).

Fluorescence microscopy

Cells were grown to logarithmic phase in MM, harvested by centrifugation, and visualized at room temperature by fluorescence microscopy as described before (Cabrera et al., 2020). Briefly, images were acquired using a Nikon Eclipse 90i microscope, an ORCA-II-ERG camera (Hamamatsu), with excitation and emission filters GFP-4050B and mCherry-C (Semrock) and image acquisition software Metamorph 7.8.13 (Gataca Systems). Processing of all images was performed using Fiji (ImageJ, National Institutes of Health) (Schindelin et al., 2012). When indicated, to cover a larger volume of the cell, z-stacks of 6 images with 0.3 µm spacing were acquired and represented in single images as maximum-intensity projections.

Protein carbonyl determination

Determination of total protein carbonyls was performed as previously described (Marte et al., 2020) from cells growing in YE (unless otherwise specified) and treated with 2.5 mM H_2O_2 for 1, 4 or 5 hours. Briefly, pellets from 50 ml cultures were washed with H_2O, resuspended in carbonylation buffer (8 M urea, 20 mM sodium phosphate buffer pH 6, 1 mM EDTA and protease inhibitors) and lysed by vortexing with glass beads during 5 minutes at 4°C. Protein extracts were incubated with 1% streptomycin sulphate (Sigma, S6501) on ice for 5 minutes and centrifuged for 5 minutes. Supernatants were recovered and protein concentration was calculated by Bradford assay and diluted to 1 µg/µl with carbonylation buffer. 100 µg of protein were incubated with 4 µl 50 mM fluorescein 5-thiosemicarbazide (FTC) (Sigma) at 30°C for 2 hours protected from light. Proteins were then precipitated with 10% trichloroacetic acid

(TCA), incubated at -20°C for 10 minutes and centrifuged 10 minutes at room temperature. Pellets were washed three times with chilled ethanol:ethyl acetate (1:1) and let to air dry. To visualize protein carbonyls by sodium dodecyl sulfate-polyacrylamide electrophoresis (SDS-PAGE), pellets were resuspended in 50 µl dilution buffer (8 M urea, 20 mM Na-phosphate buffer pH 8, 1 mM EDTA). Protein concentration was determined by Bradford assay. 5 µg of protein were loaded with 5-fold sample buffer without any dye. Gels were scanned using Typhoon 8600 Variable Mode Imager scanner (Molecular Dynamics) with a 526 nm short pass filter at 800V. Gels were then fixed and total protein was visualized by silver staining. Where indicated, protein carbonyl levels were quantified using the ImageQuant 5.2 program (GE healthcare, Little Chalfont, Buckinghamshire, United Kingdom) for carbonyls and ImageJ software for total protein.

Protein solubility assay

Isolation of the detergent-insoluble protein fractions for western blot analysis was done as described before (Cabrera et al., 2020). Briefly, cells grown in MM to the logarithmic phase were harvested and resuspended in lysis buffer A [20 mM Hepes-KOH pH 7.5, 0.5% NP-40, 200 mM NaCl, 1 mM EDTA, protease inhibitor cocktail, 1 mM PMSF and aprotinin (0.03-0.07 TIU)], and lysed with glass beads. Lysates were centrifuged at 2,000 *g*, and proteins in the resulting supernatant (Total, T) were quantified by Bradford assay. Equal amounts of protein were then centrifuged at 16,000 *g* to obtain pellet (P) and soluble (S) fractions. Supernatants (T and S) and pellets in SDS sample buffer were analyzed by SDS-polyacrylamide gel electrophoresis (SDS-PAGE) gels, followed by immunoblot analysis.

Protein extracts, Sty1-HA6His purification and immuno-blot analysis

Modified trichloroacetic acid (TCA) extracts were prepared as previously described (Vivancos et al., 2005). Native extracts were prepared by lysis of cell pellets from 50 ml cultures in 250 µl lysis buffer [10% glycerol, 50 mM Tris-HCl pH 7.5, 0.1% NP-40, 150 mM NaCl, protease inhibitor cocktail, 1 mM PMSF, aprotinin (0.03-0.07 TIU) and PhoSTOP (Roche)] with glass beads using a Mini-Beadbeater-24 (Biospec Products) for 3 cycles of 45 seconds. Lysates were then centrifuged at 16.000 *g* for 10 min at 4°C and proteins in the resulting supernatant were quantified by Bradford assay. To purify Sty1-HA6His, native extracts were prepared as described above and incubated with Ni-NTA agarose beads (Qiagen) for 2 hours at 4°C. Beads were washed 3 times with lysis buffer and purified Sty1HA6His was eluted in 20 µl SDS-sample buffer. Samples were separated by SDS-PAGE and detected by immunoblotting with monoclonal anti-GFP (Takara), polyclonal anti-Atf1 (Sanso et al., 2008), polyclonal anti-Tpx1 (Jara et al., 2007), monoclonal anti-phospho-Tyr (PY20, BD Biosciences), polyclonal anti-p38 (Cell Signaling Technology) and polyclonal anti-Sty1 antibodies (Jara et al., 2007).

RNA Extraction, Northern blot and RT-qPCR

Total RNA extraction and Northern blot were performed from logarithmically growing cells, treated or not with H_2O_2 or heat-shocked, in YE, as previously described (Vivancos et al., 2004). Transferred RNA was hybridized with α-dCTP labeled *hsp104* probe. DNase I treatment of RNA, cDNA synthesis and RT-qPCR were performed as previously described (Gonzalez-Medina et al., 2019).

Data representation: Heatmaps, Circos plot, Venn diagrams and GO clustering

Genes from YE-grown wild-type and *Δsty1* heat shocked treated cells (obtained with microarrays) (Chen et al., 2003) and genes from cells expressing Atf1.10D grown in MM (determined by RNA-sequencing) (Salat-Canela et al., 2017) were hierarchically clustered based on genes ≥2-fold up-regulated in *Δmas5* cells grown in YE (also determined by RNA-sequencing) (Vjestica et al., 2013) using Pheatmap v1.0.12, an R package to design heatmap representation (https://cran.r-project.org/package=pheatmap). To represent by Circos plot the overlap of up-regulated genes in *Δmas5* with different heat shock transcriptional programs, genes up-regulated ≥2-fold by heat-shock in wild-type cells (Chen et al., 2003) were first classified according to its dependence on Sty1 by subtracting the genes that were NOT up-regulated in a *Δsty1* background from the list of total genes up-regulated in a wild-type background. This resulted in 313 genes Sty1-dependent and 239 genes Sty1-independent (and probably Hsf1-dependent). For systematic identification, the 218 genes up-regulated ≥2-fold in a *Δmas5* strain (Vjestica et al., 2013), the 313 Sty1-dependent and the 239 Sty1-independent genes were converted to Entrez Gene ID, resulting in 187, 287 and 222 genes, respectively; those three sets of genes were finally analyzed with Metascape (Zhou et al., 2019) to yield the Circos plot. Venn diagrams were generated using the web application http://www.venndiagrams.net/. GO clusters of Biological Processes were obtained with Metascape from a single list of 160 genes coding for 160 proteins which form PACs at both 37°C and 42°C but not 30°C as determined by mass spectrometry (Cabrera et al., 2020), after converting their Systematic Gene Name

in Entrez Gene ID. The GO enrichment parameters were 3 (minimum overlap), 0.001 (P-value cutoff) and 1.5 (minimum enrichment).

Table S1. Strains used in this study, Related to Transparent Methods

Strain	Genotype	Origin
666	*h⁺ ura4D-18 leu1-32 ade6-M210*	Bioneer collection
972	*h⁻*	(Leupold, 1970)
AV18	*h⁻ sty1::kanMX6*	(Zuin et al., 2005)
AV25	*h⁻ pap1::kanMX6*	(Zuin et al., 2005)
EP198	*h⁺ ctt1::natMX6*	(Paulo et al., 2014)
EHH5	*h⁻ sty1-GFP::kanMX6 leu1-32*	(Zuin et al., 2005)
EP203.10D	*h⁻ atf1::natMX6 sty1'-HA-Atf1.10D::leu1+.*	(Salat-Canela et al., 2017)
EP48	*h⁺ pyp1::natMX6*	This work
JA578	*h⁻ sty1-HA6His::ura4+ ura4-D18 leu1-32 ade6-704*	This work
KS2088	*h⁻ sty1-HA6His::ura4+ wis1DD-12myc::ura4+ leu1-32 ura4-D18*	(Shiozaki et al., 1998)
MS98	*h⁻ atf1::natMX6*	(Fernandez-Vazquez et al., 2013)
SB234	*h⁻ mas5::kanMX6 sty1::natMX6*	This work
SB245	*h⁺ mas5::kanMX6 ctt1::natMX6*	This work
SB26	*h⁻ mas5::kanMX6*	This work
SB273	*h⁰ urg1'-hsf1::kanMX6 leu1-32 ade6-M210*	This work
SB291	*h⁻ ssa1::kanMX6*	This work
SB319	*h⁻ mas5::kanMX6 atf1::natMX6*	This work
SB464.10D	*h⁻ ctt1::kanMX6 atf1::natMX6 sty1'-HA-Atf1.10D::leu1+.*	This work
SB472	*h⁻ nmt41x'::leu1+*	This work
SB584	*h⁻ sty1-HA6His::ura4+ mas5::kanMX6 ura4-D18 leu1-32 ade6-704*	This work
SB585	*h⁻ pyp1-GFP::natMX6 ura4D-18 leu1-32*	This work
SB586	*h⁻ pyp1-GFP::natMX6 mas5::kanMX6 ura4D-18 leu1-32*	This work
SB589	*h⁻ sty1'-GFP-pyp1::leu1+*	This work
SB592	*h⁻ pyp1::kanMX6 sty1'-GFP-pyp1::leu1+*	This work
SB597	*h⁻ pyp1::kanMX6 nmt41x'::leu1+*	This work
SB598	*h⁻ mas5::kanMX6 nmt41x'::leu1+*	This work
SB605	*h⁻ mas5::kanMX6 sty1'-GFP-pyp1::leu1+*	This work
SB642	*h⁻ pyp1-GFP::natMX6 sty1'-mCherry-mas5::leu1+ ura4D-18*	This work
SB649	*h⁻ sty1-HA6His::ura4+ mas5::kanMX6 sty1'-GFP-pyp1::leu1+ ura4-D18 ade6-704*	This work
SB677	*h⁰ mas5::kanMX6 pyp1::natMX6*	This work
SB678	*h⁻ pyp1-GFP::natMX6 mas5::kanMX6 nmt41x'-mas5::leu1+ ura4D-18*	This work
SG287	*h⁺ hsp104::natMX6*	This work
SG289	*h⁻ ssa2::natMX6*	This work
SG300	*h⁻ mas5::kanMX6 hsp104::natMX6 ura4-D18 ade6-M210*	This work
SG301	*h⁻ mas5::kanMX6 pap1::natMX6*	This work
SO7701	*h⁻ urg1'-hsf1::kanMX6 mas5::ura4+ ura4-D18 leu1-32 ade6-M2x*	(Vjestica et al., 2013)

SUPPLEMENTAL REFERENCES

Alfa, C., Fantes, P., Hyams, J., McLeod, M., and Warbrick, E. (1993). Experiments with Fission Yeast: A Laboratory Course Manual (Cold Spring Harbor, N.Y.: Cold Spring Harbor Laboratory).

Bahler, J., Wu, J.Q., Longtine, M.S., Shah, N.G., McKenzie, A., III, Steever, A.B., Wach, A., Philippsen, P., and Pringle, J.R. (1998). Heterologous modules for efficient and versatile PCR-based gene targeting in Schizosaccharomyces pombe. Yeast *14*, 943-951.

Cabrera, M., Boronat, S., Marte, L., Vega, M., Perez, P., Ayte, J., and Hidalgo, E. (2020). Chaperone-Facilitated Aggregation of Thermo-Sensitive Proteins Shields Them from Degradation during Heat Stress. Cell Rep *30*, 2430-2443 e2434.

Calvo, I.A., Gabrielli, N., Iglesias-Baena, I., Garcia-Santamarina, S., Hoe, K.L., Kim, D.U., Sanso, M., Zuin, A., Perez, P., Ayte, J.*, et al.* (2009). Genome-wide screen of genes required for caffeine tolerance in fission yeast. PLoS One *4*, e6619.

Chen, D., Toone, W.M., Mata, J., Lyne, R., Burns, G., Kivinen, K., Brazma, A., Jones, N., and Bahler, J. (2003). Global transcriptional responses of fission yeast to environmental stress. Mol.Biol.Cell *14*, 214-229.

Fernandez-Vazquez, J., Vargas-Perez, I., Sanso, M., Buhne, K., Carmona, M., Paulo, E., Hermand, D., Rodriguez-Gabriel, M., Ayte, J., Leidel, S.*, et al.* (2013). Modification of tRNA(Lys) UUU by elongator is essential for efficient translation of stress mRNAs. PLoS Genet *9*, e1003647.

Gonzalez-Medina, A., Hidalgo, E., and Ayte, J. (2019). Gcn5-mediated acetylation at MBF-regulated promoters induces the G1/S transcriptional wave. Nucleic Acids Res *47*, 8439-8451.

Jara, M., Vivancos, A.P., Calvo, I.A., Moldon, A., Sanso, M., and Hidalgo, E. (2007). The peroxiredoxin Tpx1 is essential as a H2O2 scavenger during aerobic growth in fission yeast. Mol Biol Cell *18*, 2288-2295.

Leupold, U. (1970). Genetical methods for *Schizosaccharomyces pombe*. Methods Cell Physiol. *4*, 169-177.

Marte, L., Boronat, S., Garcia-Santamarina, S., Ayte, J., Kitamura, K., and Hidalgo, E. (2020). Identification of ubiquitin-proteasome system components affecting the degradation of the transcription factor Pap1. Redox biology *28*, 101305.

Paulo, E., Garcia-Santamarina, S., Calvo, I.A., Carmona, M., Boronat, S., Domenech, A., Ayte, J., and Hidalgo, E. (2014). A genetic approach to study H2O2 scavenging in fission yeast--distinct roles of peroxiredoxin and catalase. Mol Microbiol *92*, 246-257.

Salat-Canela, C., Paulo, E., Sanchez-Mir, L., Carmona, M., Ayte, J., Oliva, B., and Hidalgo, E. (2017). Deciphering the role of the signal- and Sty1 kinase-dependent phosphorylation of the stress-responsive transcription factor Atf1 on gene activation. J Biol Chem *292*, 13635-13644.

Sanso, M., Gogol, M., Ayte, J., Seidel, C., and Hidalgo, E. (2008). Transcription factors Pcr1 and Atf1 have distinct roles in stress- and Sty1-dependent gene regulation. Eukaryot Cell *7*, 826-835.

Schindelin, J., Arganda-Carreras, I., Frise, E., Kaynig, V., Longair, M., Pietzsch, T., Preibisch, S., Rueden, C., Saalfeld, S., Schmid, B.*, et al.* (2012). Fiji: an open-source platform for biological-image analysis. Nat Methods *9*, 676-682.

Shiozaki, K., Shiozaki, M., and Russell, P. (1998). Heat stress activates fission yeast Spc1/StyI MAPK by a MEKK-independent mechanism. Mol.Biol.Cell *9*, 1339-1349.

Vivancos, A.P., Castillo, E.A., Biteau, B., Nicot, C., Ayte, J., Toledano, M.B., and Hidalgo, E. (2005). A cysteine-sulfinic acid in peroxiredoxin regulates H2O2-sensing by the antioxidant Pap1 pathway. Proc Natl Acad Sci U S A *102*, 8875-8880.

Vivancos, A.P., Castillo, E.A., Jones, N., Ayte, J., and Hidalgo, E. (2004). Activation of the redox sensor Pap1 by hydrogen peroxide requires modulation of the intracellular oxidant concentration. Mol Microbiol *52*, 1427-1435.

Vjestica, A., Zhang, D., Liu, J., and Oliferenko, S. (2013). Hsp70-Hsp40 chaperone complex functions in controlling polarized growth by repressing Hsf1-driven heat stress-associated transcription. PLoS Genet *9*, e1003886.

Zhou, Y., Zhou, B., Pache, L., Chang, M., Khodabakhshi, A.H., Tanaseichuk, O., Benner, C., and Chanda, S.K. (2019). Metascape provides a biologist-oriented resource for the analysis of systems-level datasets. Nat Commun *10*, 1523.

Zuin, A., Vivancos, A.P., Sanso, M., Takatsume, Y., Ayte, J., Inoue, Y., and Hidalgo, E. (2005). The glycolytic metabolite methylglyoxal activates Pap1 and Sty1 stress responses in Schizosaccharomyces pombe. J Biol Chem *280*, 36708-36713.